The Dhaulagiri Transtensional Zone

An active fault zone within the
Western Nepal Himalaya

A Thesis

Presented to

the Faculty of the Department of Earth and Atmospheric Sciences

University of Houston

In Partial Fulfillment

of the Requirements for the Degree

Masters of Science

By

Calvin R.P. Silver

May 2012

The Dhaulagiri Transtensional Zone:

an active fault zone within the

Western Nepal Himalaya

Calvin R.P. Silver

APPROVED:

Dr. Michael Murphy, Chairman

Dr. William Dupré

Dr. Michael H. Taylor

Dr. Mark A. Smith
Dean, College of Natural Science and Mathematics

ACKNOWLEDGMENTS

My thanks go to Dr. Michael Murphy for his assistance and continued support throughout the generation of this thesis, to Dr. Michael Taylor for his knowledge and excitement in the field area, to Dr. John Goess for adding a whole new chapter onto the evolution of this study and being a great time in the field, to Dr. William Dupré for pointing me in the right direction so very early in the progress of my Masters, to Thomas Baltz for his anger and sternness throughout my geology career thus far, to Dr. Thomas Lapen for giving me my first start into true research, to Erin Page for putting up with me through two field seasons in Nepal and pushing me to do my work here at home, to my mother and father who have supported me throughout my academic career and introduced me to geology, and finally to Bhim Chand and Earth Paradise Expeditions of Kathmandu, Nepal whom made the field work for this thesis much easier through long days, heavy loads, high mountains, and challenging weather. Without Bhim and his team of porters this work would have been impossible to perform.

The Dhaulagiri Transtensional Zone

An active fault zone within the
Western Nepal Himalaya

An Abstract of a Thesis

Presented to

the Faculty of the Department of Earth and Atmospheric Sciences

University of Houston

In Partial Fulfillment

of the Requirements for the Degree

Masters of Science

By

Calvin R.P. Silver

May 2012

ABSTRACT

Field mapping and remote sensing in the Dhaulagiri Range of Nepal reveal a regionally extensive active fault zone linking the Tibrikot Fault to the Dhaulagiri Southwest Fault, herein termed the Dhaulagiri Transtensional Zone [DTZ]. Right and normally offset Quaternary features exist along the extent of the DTZ. Field investigations at key sites constrain the local geometry, kinematics, and magnitude of slip. The DTZ accommodates slip along two strike-slip faults striking N40-50W with an extensional right step-over striking N10-20E. Dextral slip is interpreted to decrease from northwest to southeast, 650 m to 450 m respectively. The DTZ is indicative of the most recent deformation processes in western Nepal, postdating other structures in the region. Oblique slip along dextral fault segments as well as linkage to dip-slip structures suggests the DTZ accommodates strain both parallel and orthogonal to the Himalayan arc. This normal/strike-slip strain is thought to be accommodated either synkinematically along the DTZ extent or cyclically with high frequency at this stage of Himalaya growth. On the basis of geometry, kinematics, and structural position we correlate the DTZ to active faulting along the Karakoram Fault, the Gurla Mandhata-Humla fault systems, and the Dhaulagiri Southwest Fault. This suggests a 350 km long right-slip fault system across the Western Nepal Himalaya. This, now contiguous, regionally extensive system lies between active north-south compression at the toe of the Himalayan thrust wedge and east-west extension in its hinterland (Tibetan Plateau). We interpret this system to

operate as a transitional margin between the differing styles of deformation. Future evolution of the system into a through-going discrete structural feature suggests the possible formation of a forearc sliver, partitioning strike-slip strain from the obliquity of convergence away from other regional dip-slip structures.

CONTENTS

INTRODUCTION

Strike-slip faulting is found at oblique convergent margins along with thrust faults and extensional domains. This strain partitioning is observed at several plate margins globally. Ocean-continent collision zones with strike-slip faulting attributed to oblique convergence are observed at (but not limited to) the island of Sumatra (McCaffrey, 1991, 2009), Taiwan between the Philippine Sea Plate and the Eurasia plate boundary (Barrier et al., 1991), the Aleutian Islands (Ekström and Engdahl, 1989), and the Peru-Chile trench (e.g. Glodny et al., 2005; Turner et al., 2007; Moreno et al., 2008; Melnick et al., 2009). Several intracontinental plate boundaries also exhibit strike-slip faulting attributed to oblique convergence, such as the Zagros Mountains (Vernant and Chéry, 2006), the Pacific-North American Plate margin of the western United States (e.g. Mount and Suppe, 1987; Zoback et al., 1987; Jackson and Molnar, 1991; Molnar, 1992; Jones and Wesnousky, 1992; Braun and Beaumont, 1995), and within the Himalayan-Tibetan Orogen (e.g. Tapponnier and Molnar, 1979; Armijo et al., 1986,1989; McCaffrey and Nábelek, 1998; Seeber and Pêcher, 1998). Structures indicative of oblique movement are active across the Himalaya Orogen amongst the classic and well documented crustal scale fault systems in the Himalayan thrust belt.

The majority of tectonic convergence between India and Eurasia, 4-5 cm/yr (Larson et al., 1999; Chen et al., 2004), is accommodated within the Himalaya via arc-normal cotractional and extensional structures (e.g. LeFort, 1975; Colchen et al., 1980, 1986; Burg et al., 1984; Yin and Harrison, 2000; Godin, 2003; Taylor and Yin, 2009; Searle et al., 2008, 2010), while strain in the hinterland of the Himalayan thrust belt is accommodated by arc-perpendicular normal faults (e.g. Armijo et al., 1986, 1989; Cogan et al., 1998; Yin et al., 1999; Yin, 2000; Taylor et al., 2003; Dewane et al., 2006; Hager et al., 2006; Taylor and Peltzer, 2006; Mahéo et al., 2007; Murphy et al., 2010; Lee et al., 2011).

In this contribution we document a regionally extensive and active right-stepping right-slip system that lies between these iconic frontal contractional and hinterland extensional structures. This system links active structures in the Karakoram Fault Zone to the Himalaya of Nepal (e.g. Nakata, 1989, 1990; Dunlap et al., 1998; Searle et al., 1998; Yin et al., 1999; Murphy et al., 2000; Murphy and Copeland, 2005; Murphy and Burgess, 2006; Styron et al., 2011). The southeastern tip of this system extends into the previously unmapped region of the Dhaulagiri Himalaya. The activity of the Dhaulagiri region is a key to understanding: 1). the relationship between the system in the northwest and the interpreted arc-normal neotectonics near Thakkhola Graben (Hurtado et al., 2001; McDermott et al., 2009), and 2). how this activity is related to the differing kinematics of frontal compression and hinterland extension, as well as regional scale orogenic growth.

ACTIVE STRUCTURES WITHIN THE NEPAL HIMALAYA

The Himalayan Orogen is the product of collision between India and Eurasia. The Main Frontal Thrust [MFT] is the primary active shortening structure, accommodating ~2 cm/yr of convergence (Lavé and Avouac, 2000). Late Quaternary deformation near the toe of the Siwalik Sub-Himalaya denotes the MFT and the margin between India-Eurasia (Nakata, 1975; Malik and Nakata, 2003). North of the MFT are crustal scale thrusts spanning the length of the Himalayan Orogen. Structurally above the

MFT is the Main Boundary Thrust [MBT], likely a steep thrust; it separates the Siwalik Sub-Himalaya from the low grade metapelitic Lesser Himalaya Crystalline [LHC] rocks (Schelling, 1992). The MBT shows evidence of motion in the Quaternary and thermochronology suggests activation >10 Ma, making it an active and long-lived structure (Miegs et al., 2005). The Main Central Thrust [MCT] marks the boundary between the LHC and the Greater Himalayan Crystalline [GHC] rocks. The MCT is interpreted to have accommodated 80-100 km of crustal shortening between 22 and 18 Ma (Hubbard, 1989). In general the MCT is interpreted to have ceased movement in the Middle Miocene (Vannay and Hodges, 1996; Carosi et al., 2007). The South Tibetan Detachment System [STDS] lies structurally above the MCT and separates the GHC rocks in the footwall from the Tethyan Sedimentary Sequence [TSS] in the hangingwall. This north-dipping structure is thought to have initiated as early as 22 Ma (Hodges et al., 1992; Brown and Nazarchuk, 1993; Coleman, 1996; Godin et al., 1999).

Recent slip along the MCT and STDS has been interpreted near the southern end of Thakkhola Graben between the Dhaulagiri and Annapurna Himalaya (Figure 1). Muscovite $^{40}Ar/^{39}Ar$, apatite fission track, and ^{10}Be age discontinuities specially correlate with observed steepening of river gradients along the Annapurna Front (Wobus et al., 2003, 2005; Hodges et al., 2004). This change straddles mapped segments of the MCT suggesting slip along the MCT between 4 Ma to present.

West of the Annapurna Himalaya, recent slip along the STDS has been interpreted near the southern end of the Thakkhola Graben on the south shoulder of Dhaulagiri I.

Figure 1. Map of structures active in and around the Himalaya of Nepal since the Oligocene. KRM-Karakoram Fault Zone, LGS-Lunggar Shan, LKG-Lopukangri, GM-H-Gurla Mandhata-Humla Fault System, TKG-Thakkhola Graben, BGF-Bari Gad Fault, DSWF-Dhaulagiri Southwest Fault, MBF-Main Boundary Fault, MFT-Main Frontal Thrust. 1-Murphy and Burgess, 2006, 2-Murphy and Copeland, 2005, 3-Nakata, 1989, 1990, 4-Styron et al., 2011, 5-McDermott et al., 2009, 6-Hurtado et al., 2001, 7-Hodges et al., 2004, 8-Wobus et al., 2003, 2005. Note: Gap in established structures near the Dhaulagiri Himalaya; transition from N-S compression to E-W extension; distinct oblique chain of structures between foreland and hinterland.

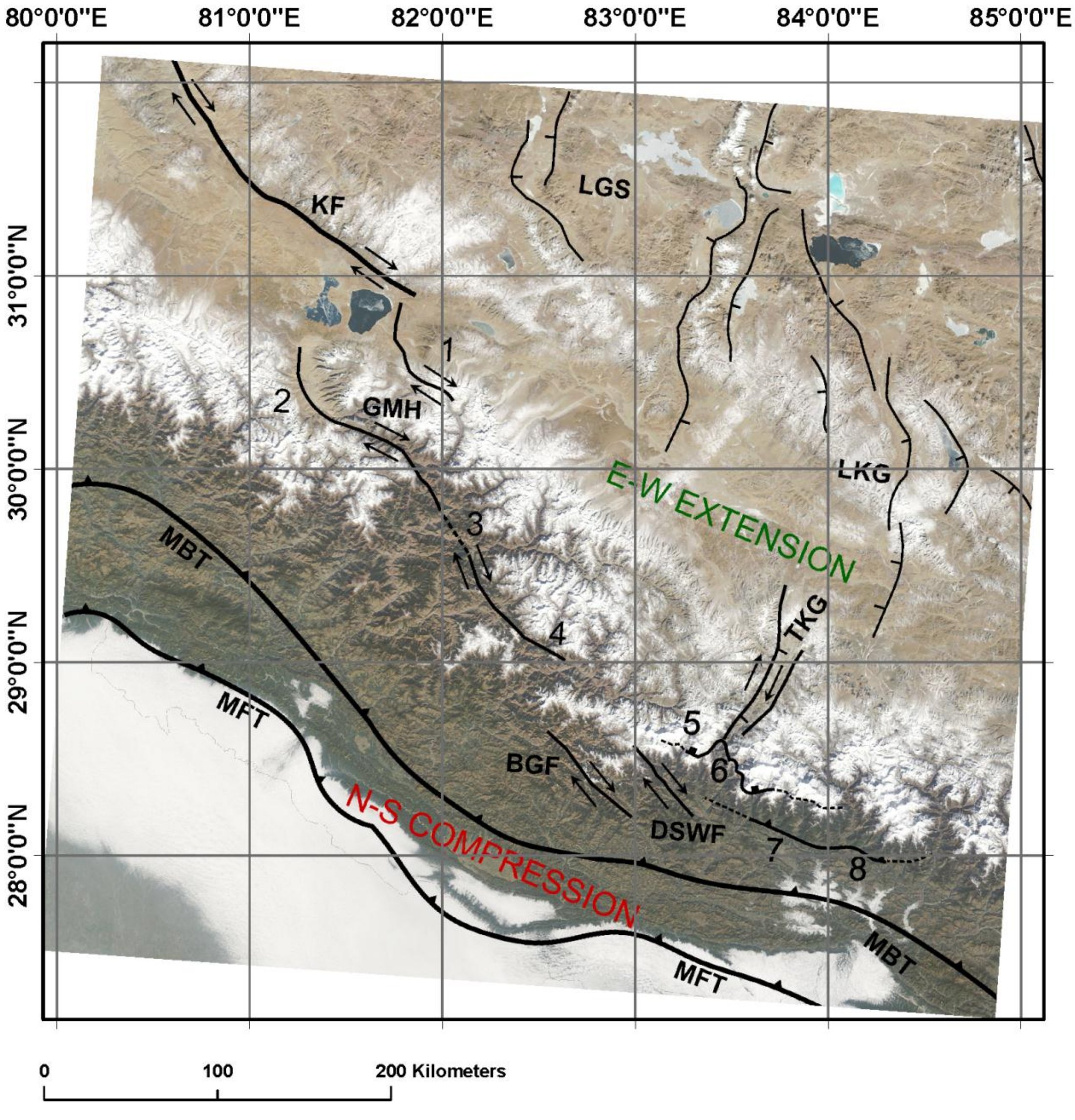

80°0'0"E
81°0'0"E
82°0'0"E
83°0'0"E
84°0'0"E
85°0'0"E
31°0'0"N
30°0'0"N
29°0'0"N
28°0'0"N
KF
LGS
1
2
GMH
E-W EXTENSION
LKG
3
MBT
4
TKG
MFT
5
BGF
6
N-S COMPRESSION
DSWF
7
8
MBT
MFT
0
100
200 Kilometers

Structural relationships documented by Hurtado et al. (2001) suggest the Dangardzong Fault, on the west side of Thakkhola Graben, terminates against the Dhumpu Detachment within the STDS zone. Offset river terraces across the Dangardzong Fault were radiocarbon dated at 17.2 ka. This constrains the Dhumpu Detachment to have been active within the last 17.2 ka.

The Hurtado et al. (2001) study alluded to a potential connection via a shear zone across the south flank of Dhaulagiri I between the Dhumpu Detachment and the Dhaulagiri Southwest Fault [DSWF], an active structure first mapped by Nakata (1989, 1990). This DSWF was originally mapped as a right-slip fault, though the Hurtado et al. (2001) study interpreted the fault to accommodate normal slip.

McDermott et al. (2009) interpret the presence of the 15-20˚ north-dipping Larjung Detachment in the Kali Gandaki and Myagdi Valleys within the Dhaulagiri Himalaya STDS zone. The detachment is expressed as a 1-10 m thick brittle-ductile shear zone within the TSS structurally above the interpreted Dhumpu and Annapurna Detachments (Hurtado et al. 2001). Ductile fabrics in this shear zone indicate normal and right-lateral slip. (U-Th)/He apatite cooling ages indicate exhumation of its footwall at <3.4 Ma, which is interpreted to reflect slip along the detachment at that time.

The Larjung, Dhumpu, and Annapurna Detachments are interpreted to be western extensions of the Machhapuchhare and Phu Detachments in the Annapurna Himalaya (Hurtado et al., 2001; McDermott et al., 2009). The westward continuation of the Larjung Detachment suggests the presence of modern oblique motion in the relatively unmapped western Dhaulagiri Himalaya.

North of these north-dipping Himalaya faults is the Tibetan Plateau. While convergent systems are dominant near the Himalaya Front, the current deformation in Tibet is characterized by north striking normal fault systems accommodating east-west extension. With few exceptions, extensional fault systems in the Tibetan Plateau do not extend southwards into the Himalaya. The most pertinent systems to this study of the western Nepal Himalaya are the Lunggar Shan and Lopukangri fault systems (Kapp et al., 2008; Taylor et al., 2007; Murphy et al., 2010; Sanchez, 2011).

In southwestern Tibet east-west extensional domains in the plateau and north-south shortening domains in the Himalaya, are separated by the Karakoram Fault Zone. A series of right-stepping dextral structures stem from the Karakoram transferring slip into the western Himalaya of Nepal. The Karakoram Fault in the Mt. Kailas region is estimated to have >50 km of dextral slip (Searle, 1996; Murphy et al., 2000; Murphy et al., 2002; Lacassin et al., 2004) which is estimated to have occurred since the Middle Miocene (Murphy et al., 2000; Phillips et al., 2004;). Geologic mapping shows that a significant portion of dextral strain is transferred eastward into the High Himalaya along a system of right-stepping dextral faults (Ratschbacher et al., 1994; Lacassin et al., 2004; Murphy and Copeland, 2005; Murphy and Burgess, 2006). Several faults displaying Recent right lateral separation have been identified in western Nepal and include the Tibrikot and Dhaulagiri Southwest Faults [DSWF] (Nakata, 1989, 1990; Styron et al., 2011). This study documents a previously unrecognized fault linking the Tibrikot Fault to the Dhaulagiri Southwest Fault herein referred to as the Dhaulagiri Transtensional Zone [DTZ] (Figure 2).

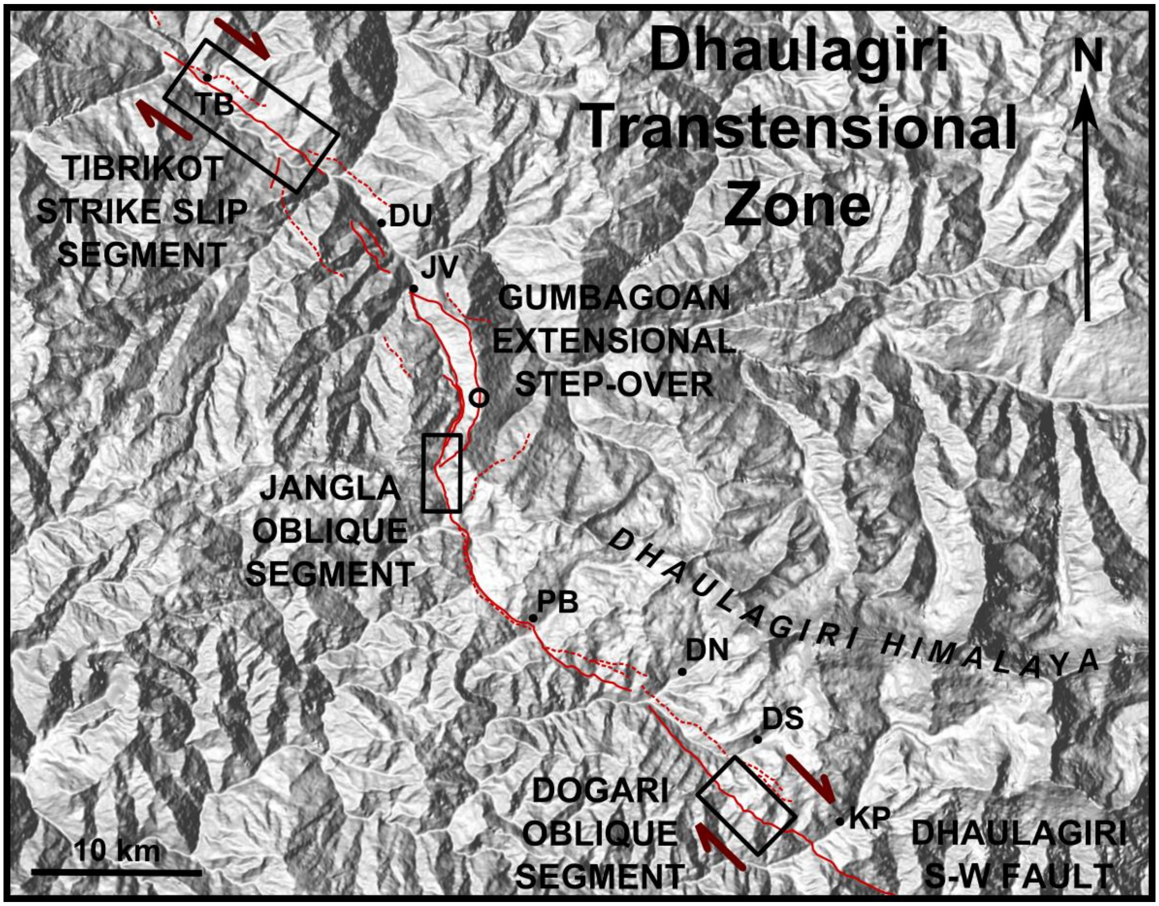

Figure 2. SRTM Image of the western Dhaulagiri Range of Nepal. Field mapped traces are in solid red. Traces interpreted from remote sensing are dotted red. Four neotectonic study sites are highlighted in white along the length of the trace, the Tibrikot Strike-slip Segment, the Gumbagoan Extensional Step-over, the Jangla Oblique Segment, the Dogari Oblique Segment. The trace of the Dhaulagiri Southwest Fault is linked to the Dhaulagiri Transtensional Zone. TB-Tibrikot, DU-Dunai, JV-Jangla Valley, PB-Purbang Valley, DN-Dogari North, DS-Dogari South, KP-Kape Valley.

THE DHAULAGIRI TRANSTENSIONAL ZONE

The DTZ was investigated at four primary sites, the Tibrikot strike-slip segment, the Gumbagoan extensional step-over, the Jangla oblique segment, and the Dogari oblique segment.

Tibrikot Strike-slip Segment

The Tibrikot segment is 12 km long and strikes N50-55W through the Lesser and Greater Himalayan rocks. It is best expressed between the villages of Tibrikot (29° 1'31.55"N, 82°47'16.33"E) and Suligad (Styron et al., 2011). The fault trace truncates and dextrally offsets south flowing streams (Figure 3). Fault slip data indicate a dominant dextral slip component of the displacement (Styron et al., 2011).

Stream offsets show dextral separations of A: 430 m, B: 634 m, C: 186 m, D: 138 m, E: 724 m, and F: 808 m (Figure 3: from west to east respectively). These measurements were calculated from GeoEye satellite images by extrapolating undeformed reaches of streams to the interpreted fault surface trace. Uncertainties exist in these offsets due to channel erosion, interpretation, and the possibility of preexisting bedrock structure. Before error could be properly assessed, the two least incised streams, C and D (Figure 4), were disregarded as they are geomorphically dis-similar to the other streams. Using streams A, B, E, and F from Figure 4, an average was calculated. The difference between this average and the largest outlying value becomes a measure of the error. The average observed dextral separation of streams A, B, E, and F with error is 649 ± 219 meters. We interpret this measurement to represent the magnitude of strike-slip since the inception of stream incision.

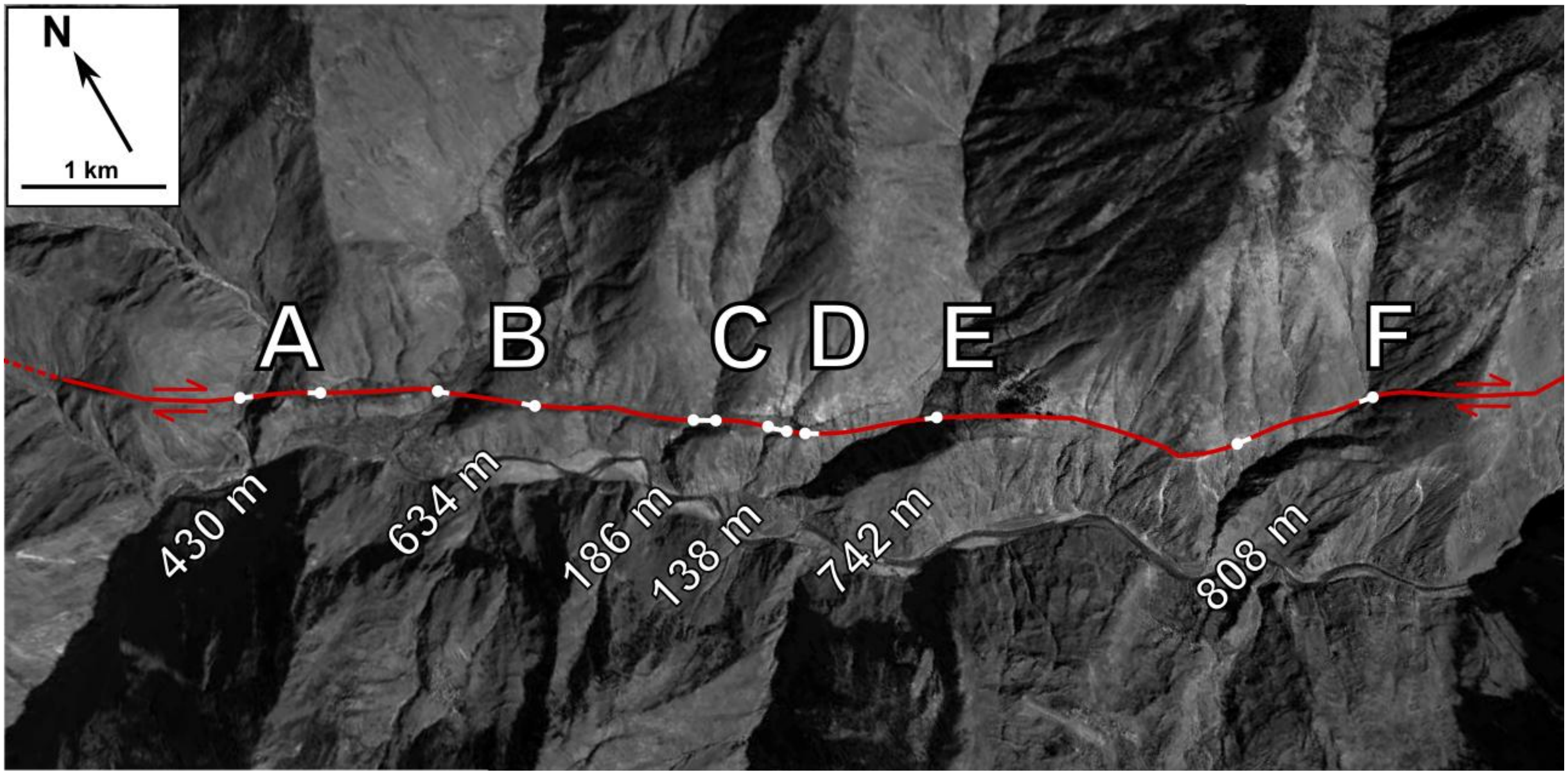

Figure 3. Satellite image of the Tibrikot Segment exhibiting the six primary offset stream and ridge sets. Measurements presented are from extrapolation of straight reaches up and downstream from the interpreted fault trace.

Figure 4. Field photo of the Tibrikot Segment taken from the air. Terraced fields are visible along the strike of the trace. Offset drainages C, D, and E are visible in this photo, corresponding to Figure 3.

View ~Due E
D
E
E'
C
514 m
D'
C'

Gumbagoan Extensional Step-over

The southeast extent of the Tibrikot Fault is difficult to discern in satellite imagery due to heavy forest growth. However, field mapping in the around Dunai Village shows a distributed system of scarps with a more north-south strike. A bifurcation exists at the mouth of Jangla Valley (Figure 2: JV). The western bifurcation strikes up Jangla Valley while the other strikes up the eastern hillside and along the ridge between Jangla Valley and the village of Gumbagoan to the east.

We interpret the scarps in Jangla Valley to be relatively young because surfaces cut by the fault traces have thick arboreal growth while the free faces have minimal shrub growth with no trees (Figure 5).

The traces along the ridge rise above tree line 12 km southeast of Tibrikot and extend for ~10 km striking N10-20E, sub-perpendicular to the Tibrikot Segment (28°51'6.49"N, 82°57'4.71"E). Along the crest of the ridge the Gumbagoan scarps are anastomosing and distributed over half a kilometer in width. The scarps cut soils and sediments consisting of poorly sorted sand-to-boulder sized clasts. Large angular clasts are abraded and may have been deposited via landslides. The cut alpine surfaces are capped by several centimeters of periglacial loess growing fine grasses, scant flowers, and small twiggy bushes above tree line (Figure 6).

The scarp faces are exposed soil and rock composites with curved surface traces. The mapped scarp network is shown in Figure 7. The primary western fault scarp shows maximum displacement of 10 m with a prominent displacement gradient along strike. Numerous splays branch off this primary scarp into distributed zones of strain with as little as 0.2 m of displacement on minor scarps. These smaller scarps also exhibit displacement gradients along strike. Field mapping of this anastomosing scarp network and their heights was performed (Figure 7).

Transects across the scarp network were generated to quantify throw (Figure 8). The scarps in the east have rounded crests and prominent colluvial wedges. Eastern scarps have more decomposed profiles, often covered with a fine carpet of grass. In the west scarps have sharp crests, planar faces, and minor colluvial wedge development (Figure 9). Moreover, the western scarps show the least amount of alpine grass growth, sometimes none. This can be clearly seen in the dip profiles shown above in Figure 8.

Several Quaternary surficial deposits are either crosscut or are generated by the Gumbagoan scarp network. There are debris flows and solifluction lobes oriented sub-perpendicular to the fault system on a 22˚ slope into the western Jangla Valley (Figure 6). These deposits are normally offset by the most westerly fault traces. Very little to no dextral separation is observed in the offset features. Water catchments have developed against uphill facing scarps. Despite these small ponding events the colluvial wedges are still fresh and have not yet developed drainage incision.

The largest scarp, 10 m, shows two slopes, the upper slope being ~30˚ and the lower slope being ~40˚ (likely related to colluvial wedge development, as well as a differential growth pattern on the free-face of the exposure (Figure 9). Midway down the scarp there is a clear change from dense shrub growth on top to little growth on bottom. This is potentially derived from multiple slip events or the commencement of a colluvial build up.

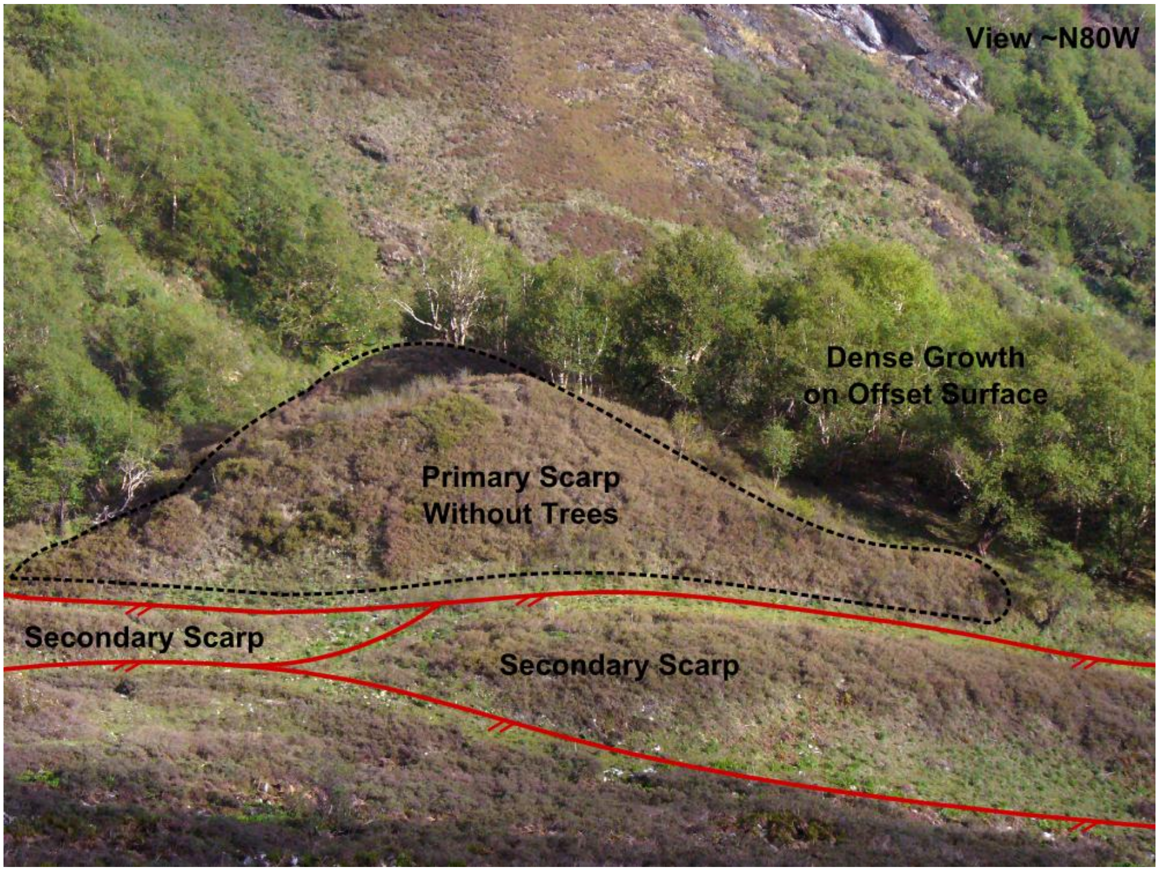

Figure 5. Field photo of scarp faces with limited growth and multiple traces cutting heavily vegetated surfaces southeast of Tibrikot. Note: differential growth of scarps and cut surfaces.

Figure 6. Field photo of the Gumbagoan Segment near the pass from the village of Gumbagoan into Jangla Valley. Distributed and anastomosing fault traces in red, cut Quaternary debris flow and minor drainages with western transport direction, ponding has occurred near one of the larger scarps.


View ~N10E

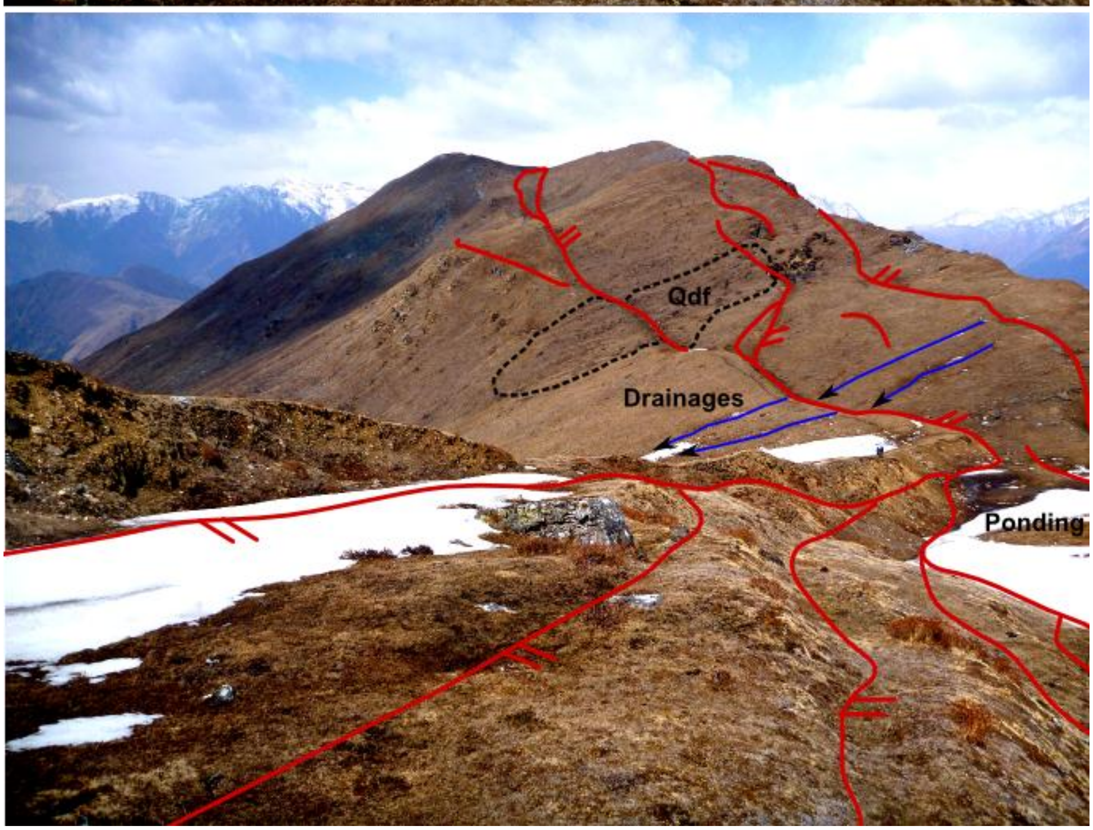
Qdf
Drainages
Ponding

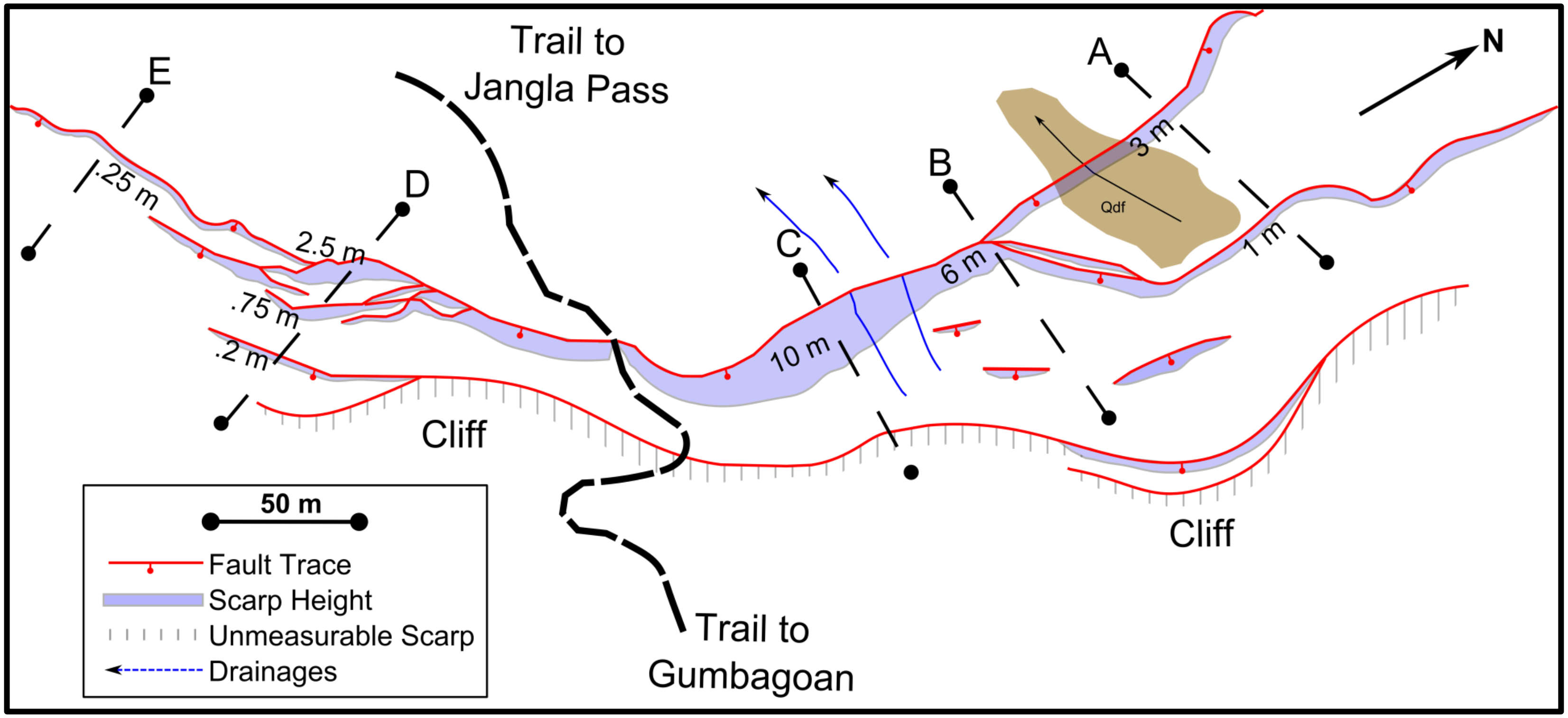

Figure 7. Trace map of the Gumbagoan Extensional Step-over near the pass from Gumbagoan into Jangla Valley. East dipping fault traces are in red. Blue represents measured height of the exposed scarp along strike with height values listed. Cliffs are interpreted to be fault related but immeasurable due to slumping down slope toward Gumbagoan. The cut Quaternary debris flow and drainages are also mapped in relation to Figure 6. Transects A-E are exhibited in Figure 8.

Figure 8. Fault profiles with locations shown in Figure 7. All transects are aligned to the primary scarp trace. Secondary traces are evident on A, C, and D. The largest discrete scarp is 10 meters in profile C. Note: the similarity in dip of surfaces disrupted by the scarps, the lack of prominent colluvial wedges in profiles B and C, the diffuse scarp profiles in A and E. C represents the most discrete scarp of the Gumbagoan Segment, E represent measurements from the most distributed scarps.

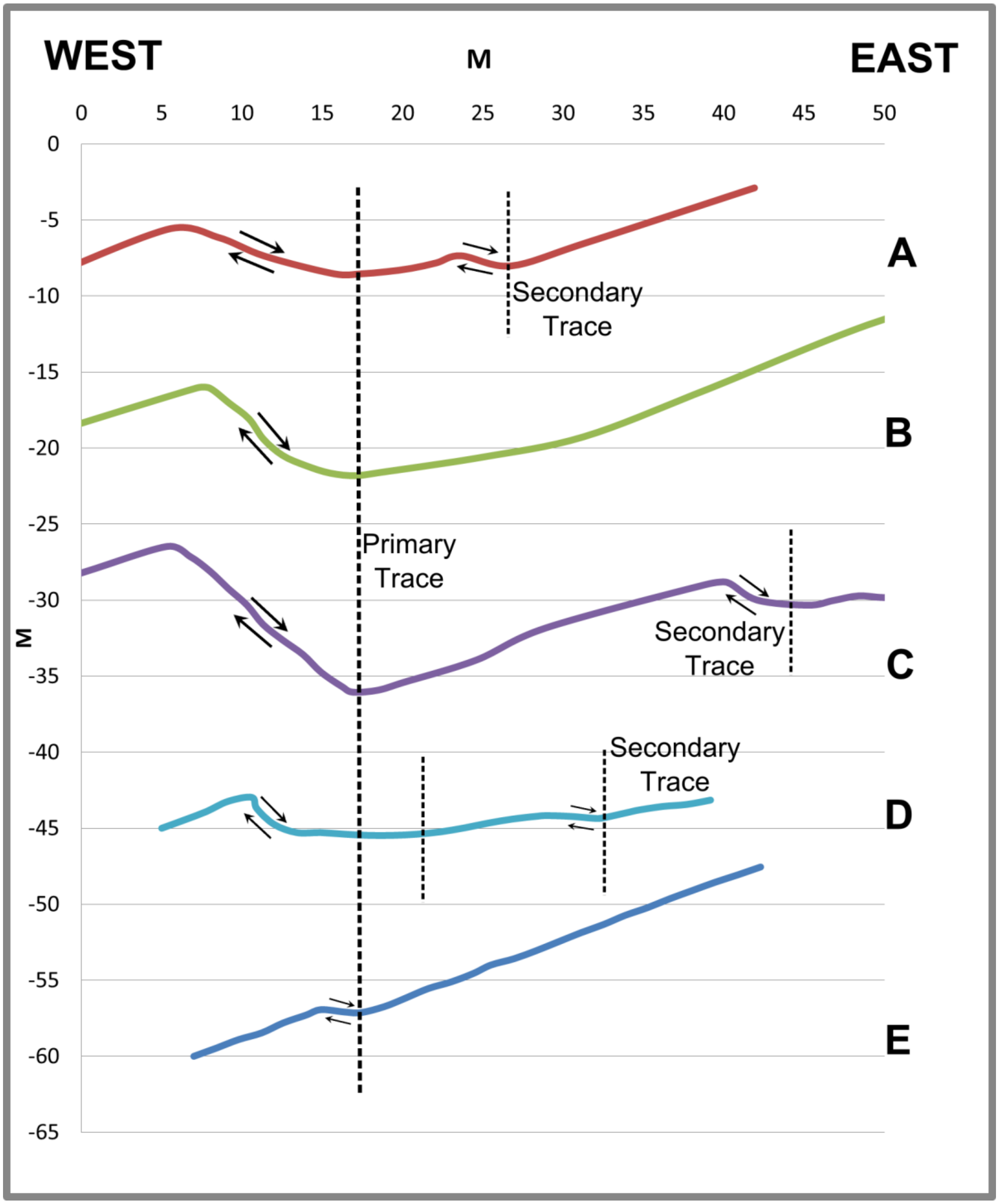

WEST
M
EAST
0
5
10
15
20
25
30
35
40
45
50
0
-5
-10
-15
-20
-25
-30
-35
-40
-45
-50
-55
-60
-65
M
A
B
C
D
E
Secondary Trace
Primary Trace
Secondary Trace
Secondary Trace

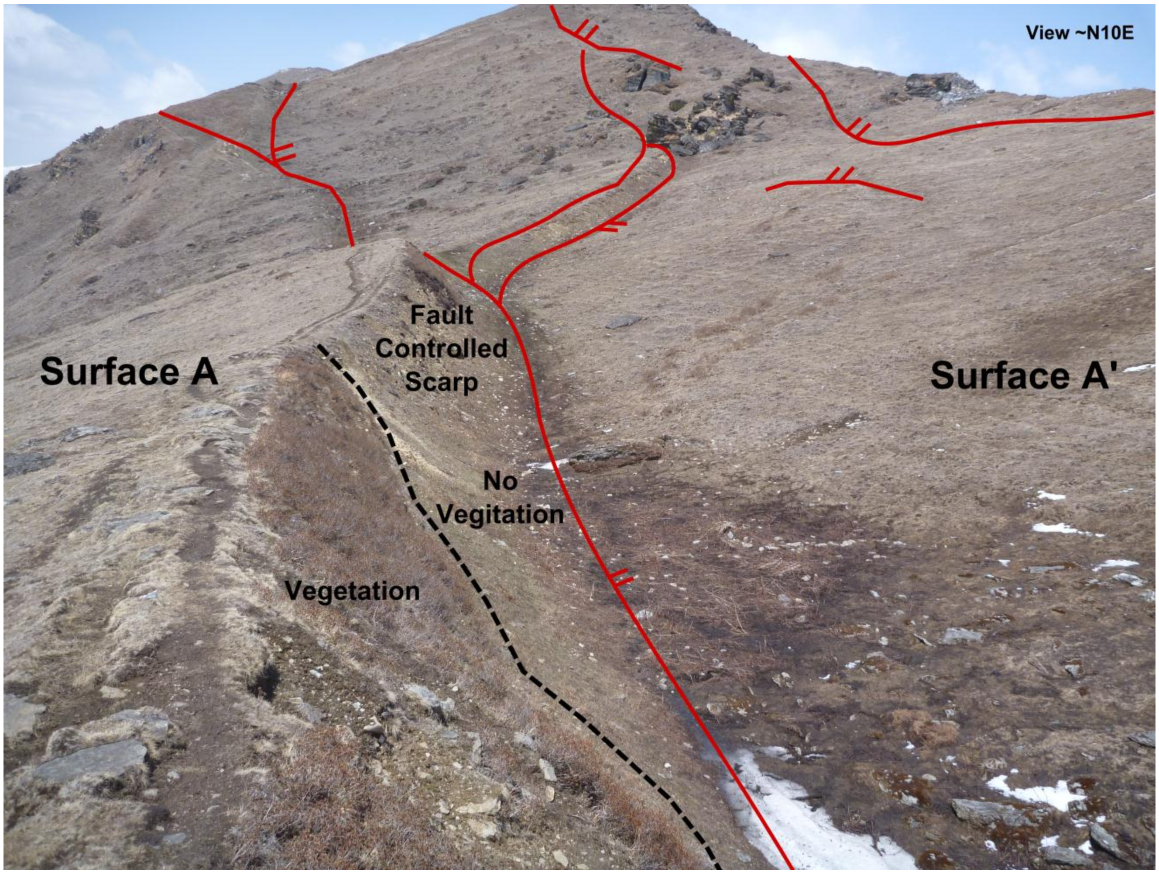

Figure 9. Field photo along strike showing the fault showing the largest discrete segment of scarp with its steep fault controlled face and the cut 'A' surface having similar dip and surficial deposits. Fault traces are in red. Differential growth domains are noted on the scarp surface.

Along 1 km of the Gumbagoan system the fault dips westward rather than eastward. A change in dip is often indicative of developing systems accommodating primarily dip-slip motion (Griffiths, 1980; Walsh and Watterson, 1991).

1 km to the west, the sub-parallel extensional system in the adjacent Jangla Valley has similar trace geometry, N10-20E with east-dipping scarps. The kinematics at this location is unknown due to vegetation and Quaternary cover.

Jangla Oblique Segment

The western and eastern segments of the Gumbagoan system merge near Jangla Bhanjyan Pass 3.5 km to the south (28°49'39.67"N, 82°55'37.63"E). We define the Jangla Oblique Segment as the fault trace network between Jangla Bhanjyan Pass and Purbang Valley. The Jangla Oblique Segment strikes ~N20W and is characterized by a 0.5 km wide zone of deformation. This network retains a distributed nature but with a straighter fault trace (Figure 10). This segment again crosscuts unconsolidated soils of periglacial loess but with a higher content of imbedded rock debris. Other sub-parallel traces are observed outside the main deformation zone.

The main segment is comprised of scarps with sharp crests and planar faces (Figure 11). The largest scarps have rerouted drainages causing erosion of the colluvial wedges throughout the area. The largest observed scarp in the valley is 2.5 meters but unknown amounts of river incision make the value a maximum.

Quaternary right separations are visible along this segment. Alluvial fans, debris flows, and drainage systems have been obliquely offset by dextral/normal faults.

Figure 10. Satellite image of the Jangla Bhanjyan Pass region. The two systems leading into the pass from the north are the Jangla Valley segment (west) and the Gumbagoan Segment (East). South of the pass is the Jangla Oblique Segment. Distributed and anastomosing fault traces in red, all east dipping. Dextral shear is interpreted on total distributed zone with varying magnitude. Inset Figure 12 is boxed.

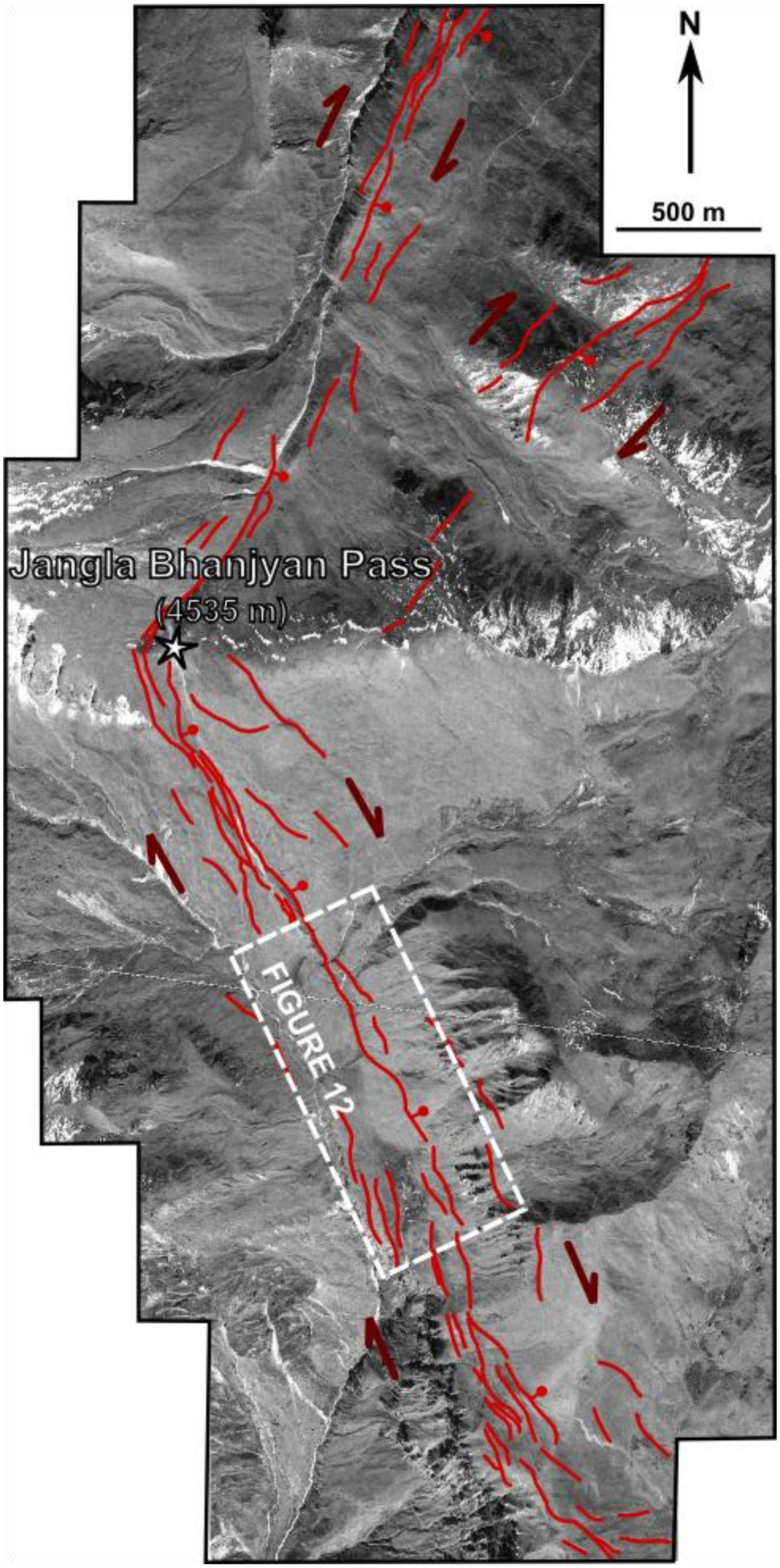

N
500 m
Jangla Bhanjyan Pass
(4535 m)
FIGURE 12

Figure 11. Field photo of the Jangla Oblique Segment leading south from the Jangla Bhanjyan Pass. Anastomosing traces in red with dextral and normal kinematics interpreted. Erosion in the valley base has generated a fault-line scarp. Surface A and A’ are interpreted to be similar and cut by fault traces.

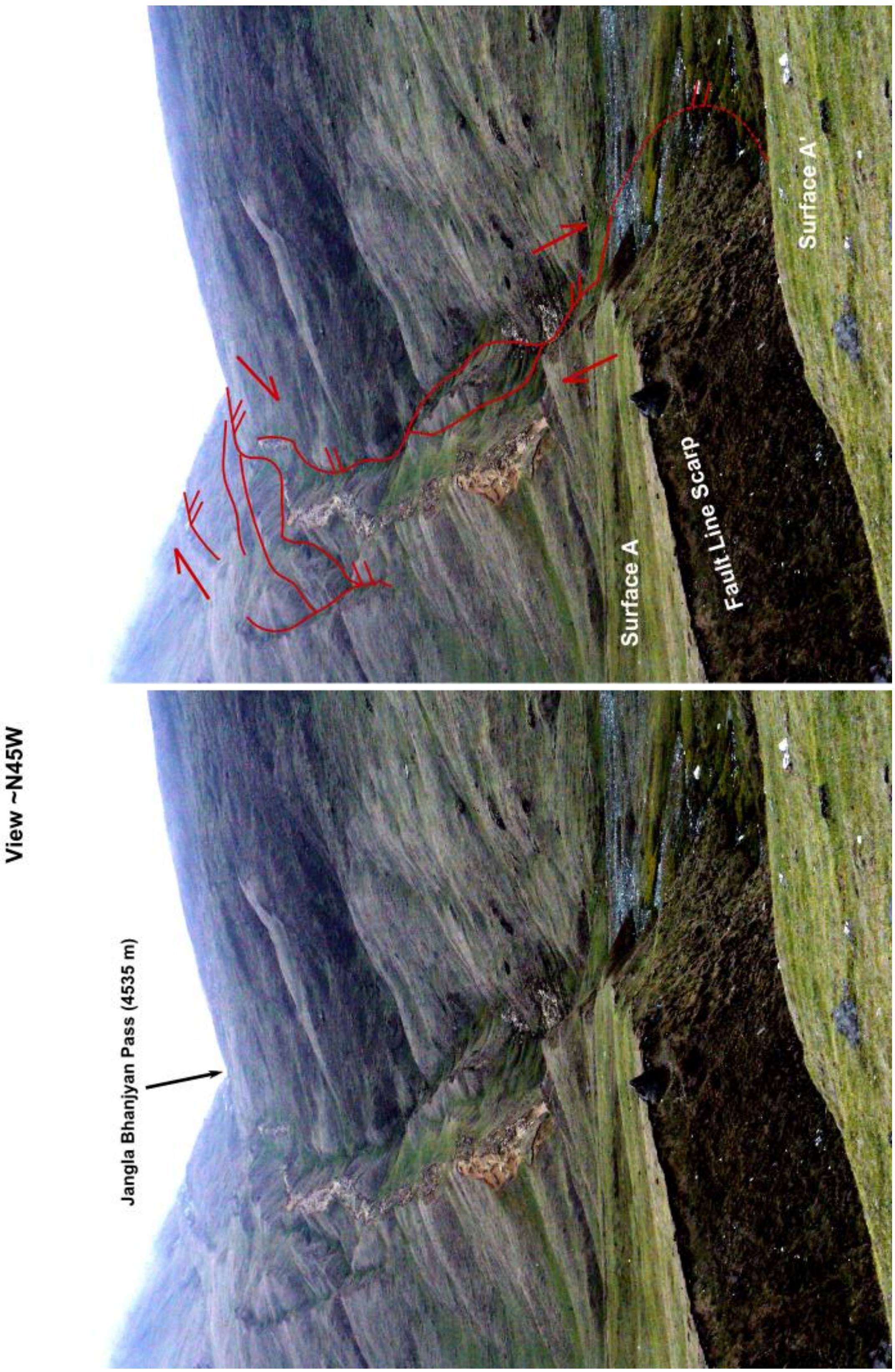
View ~N45W
Jangla Bhanjyan Pass (4535 m)
Surface A
Fault Line Scarp
Surface A'

There are landslides and alluvial fans of varying size along the northeastern wall of the valley (Figure 12). The largest active fan, sloping perpendicular to the fault scarps, exhibits dextral offset at both of its margins. Adjacent to this fan are two smaller deposits which also exhibit dextral offsets. While this offset is evident in satellite imagery the fans merge with smaller drainages and are covered with landslide, making offsets difficult to measure.

Below the pass, at the northern edge of the valley, the primary faults interact with alpine drainages flowing east-northeast to west-southwest (Figure 12). The incised and cut surfaces are interpreted to be equivalent based on observed similar loess and boulder deposits as well as similar slopes at undeformed locations. While these tributaries exhibit an apparent sinistral separation in map view the field correlation of river terraces using deposit angle, height, and morphology of incision is more consistent with a dextral slip. These terrace risers preserve evidence consistent with two right laterally offset streams. This is corroborated by the observation of ponding features, beheaded drainages, and redirected streams which is expected in the dextral offset of a two stream system.

By correlating the offset terrace risers we estimate a dextral offset of 72 m (Figure 13). However, due to erosion by the migrating streams this measurement is subject to error related to the width of the incised channels which bound the terrace treads (Figure 13). We calculate this error to be ± 9 meters.

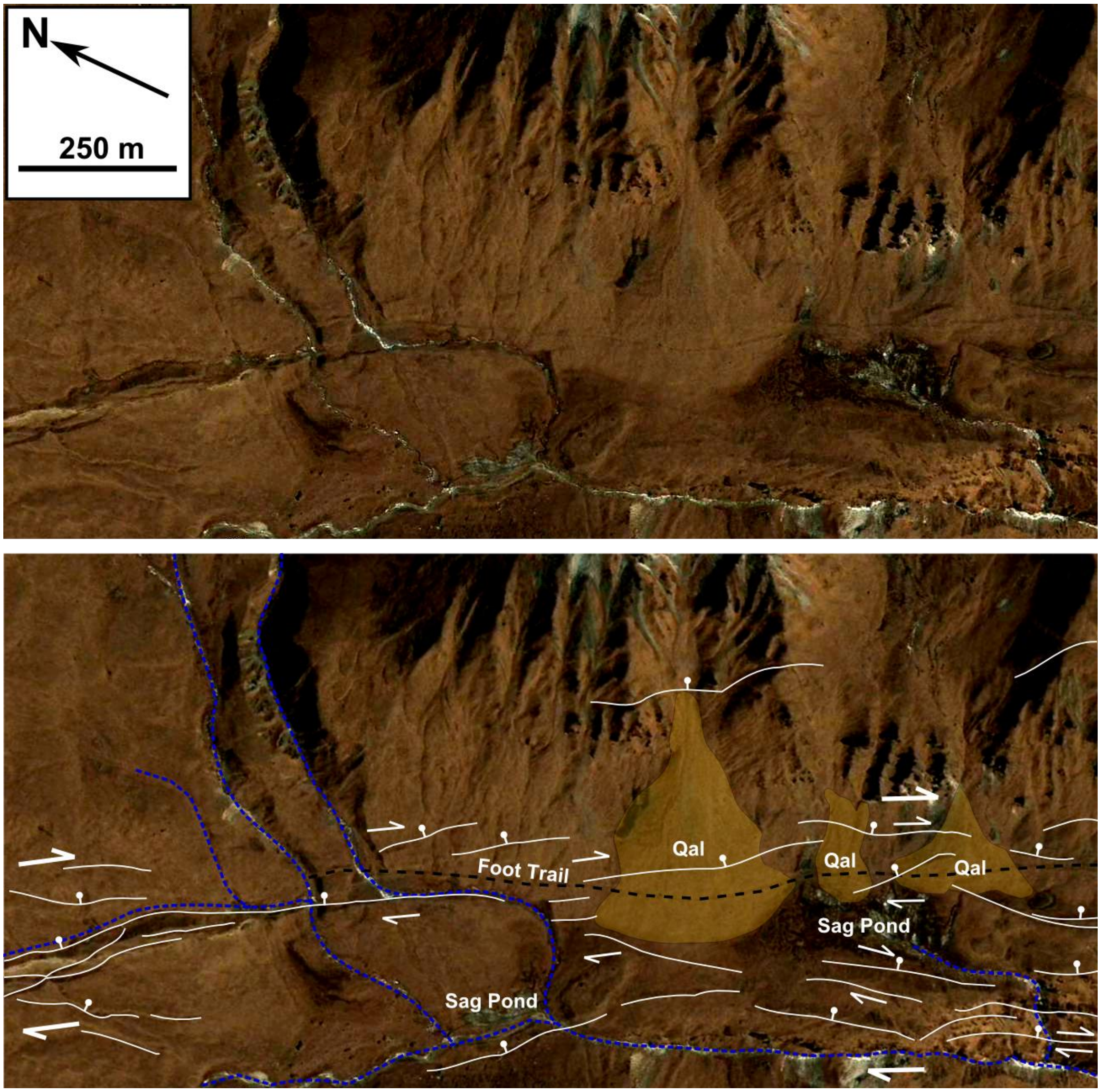

Figure 12. Inset satellite image of the Jangla basin. Fault traces are in white and all dipping northeast with dextral shear. Blue denotes drainages. Quaternary alluvial fans and sag ponds are prominent on the southern side of the basin. Note: Apparent left offset of northern drainages, dextral offset of alluvial fan margins, ponding between zones of distributed dextral motion, foot trail running along the eastern wall of the valley (not a fault trace).

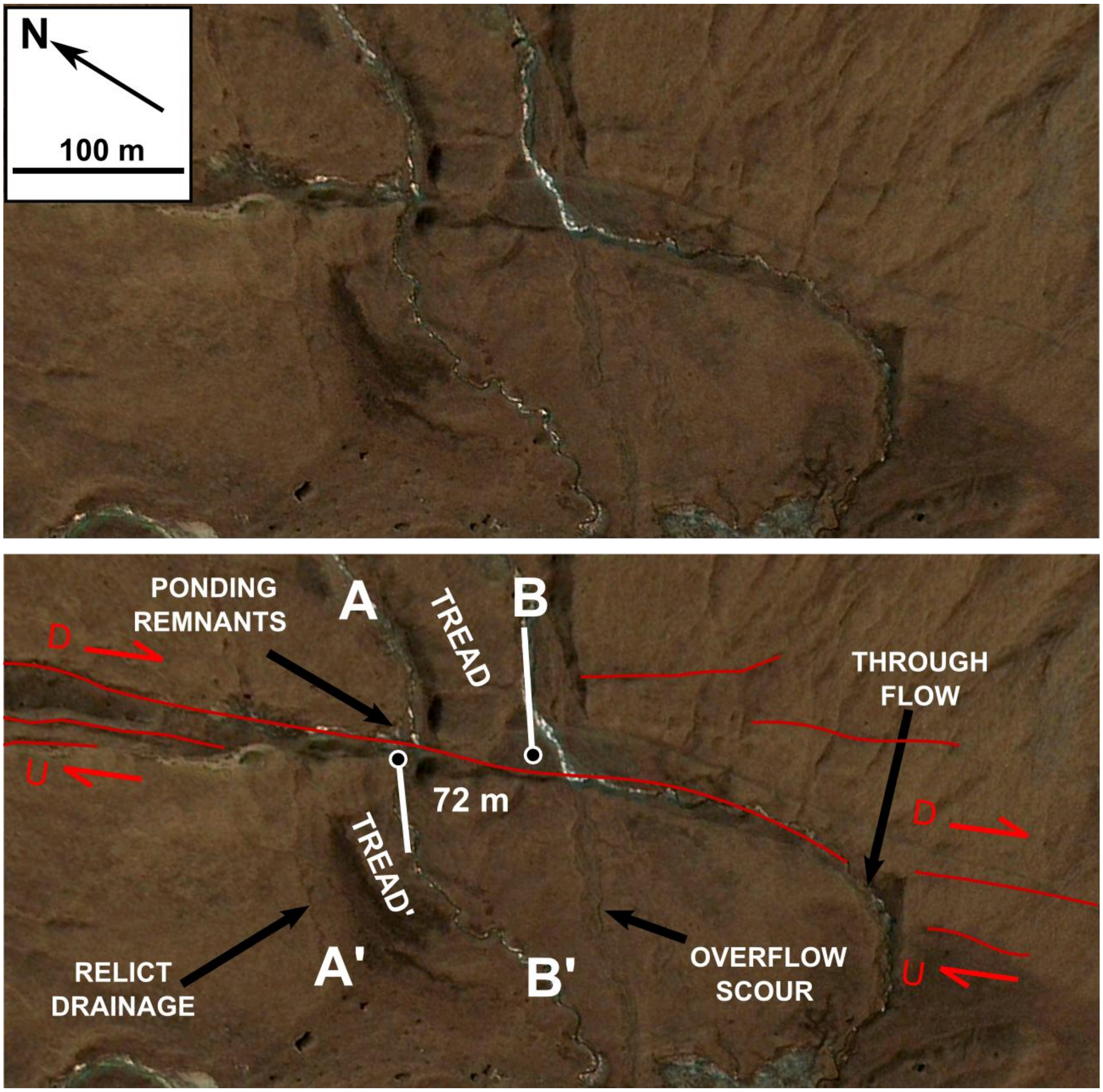

Figure 13. Satellite image of the offset river systems with fault traces in red, interpreted measuring points for offset river terraces (72 m) between streams A and B, and important geomorphic features to note. D-downthrown, U- up thrown. Evolution of this system to present morphology is modeled in Figure 14.

A simplified interpretation of how this stream morphology evolved is shown in Figure 14. Depicted is a two stream system which is crosscut by a dextral strike-slip fault with minor normal offset. Figure 14 shows two streams, A and B, of sub-equal stream width incising a high alpine plane sloping at 20˚. Between the river incisions resides a tongue shaped terrace tread which will later be used for estimating total slip.

Initiation of faulting forces dog legging of the streams, causing asymmetrical erosion of the separated terrace risers and increased incision of the up thrown side. There is a critical distance of separation between the streams and their downthrown continuations.

Once this critical separation is reached it is easier for stream A to pond against the fault scarp, subsequently rerouting to B'. Stream B ponds and moves along scarp as it has no other immediate outlet. A' goes dry and becomes a relict streambed. The previously linked terrace treads are now separated by a dry river bed which once linked stream B to B'. Note the apparent left slip of stream A-B' despite the right-slipping fault.

Ponding subsides as incision between A and B' becomes more conducive to flow. If stream B floods there will be overflow scouring on the up thrown surface adjacent to its bend along scarp. As flow continues, stream B eventually finds a point of incision along the scarp and generates a new path. This explains the development of the system we observe (Figure 13).

Figure 14. Simplified model of two stream system being offset by an oblique fault. 14-1. Two streams incising to generate a tread between them on a 20˚ dipping slope. 14-2. Oblique motion initiates and streams A and B are rerouted. Erosion of middle tread begins asymmetrically. 14-3. At a critical separation ponding will occur as through flow is becomes difficult for both streams. Stream A will deviate from A' and reroute to B'. Stream B will abandon B', pond and flow along the scarp. If the ponding B floods there will be flow over the scarp. 14-4. Present day morphology. Stream A has incised and ponding no longer occurs. A' is completely dry. Overflow scour is seen across the fault from where it has cut through the scarp at a different location. This corresponds to Figure 13.

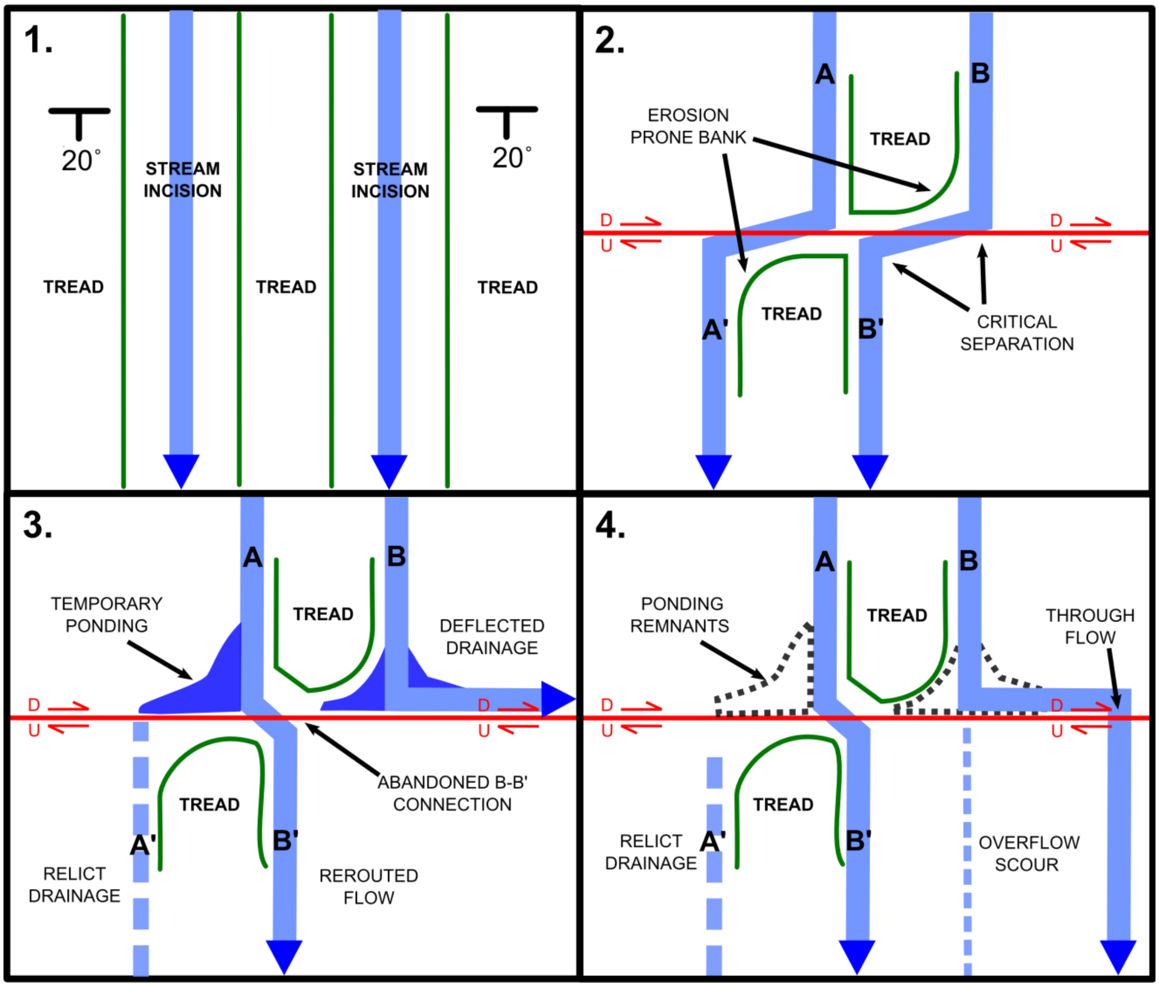
1.
20°
STREAM INCISION
TREAD
STREAM INCISION
TREAD
20°
TREAD
2.
A
B
EROSION PRONE BANK
TREAD
D
U
D
U
TREAD
A'
B'
CRITICAL SEPARATION
3.
A
B
TEMPORARY PONDING
TREAD
DEFLECTED DRAINAGE
D
U
D
U
ABANDONED B-B' CONNECTION
TREAD
A'
B'
RELICT DRAINAGE
REROUTED FLOW
4.
A
B
PONDING REMNANTS
TREAD
THROUGH FLOW
D
U
D
U
TREAD
RELICT DRAINAGE
A'
B'
OVERFLOW SCOUR

At Purbang Valley on the southeast edge of the Jangla Oblique Segment all faults merge. From Purbang southward the fault scarp is visible at ground level and in satellite imagery as primarily a single fault, although two and three faults are seen over short segments. This trace can be followed 15 km into the Dogari Block just south of the Dogari Himal and Putha Hiunchuli in the Dhaulagiri Range. Along this segment the strike changes orientation from N10-30W to N50W near Dogari with distinct “V”ing across valleys indicating the fault dips to the NNE. The orientation of this fault, as it enters Dogari, is similar in strike to the Tibrikot Segment.

Dogari Strike-Slip Segment

Inside the Dogari Block the trace is lost for an ~2 km-long stretch. The trace resumes on the south side of the river and crests the ridge between south Dogari Valley and Kape Valley to the east. The fault trace strikes ~N50W as it reaches the ridge (28°40'9.13"N, 83° 5'19.11"E). Satellite imagery shows several possible bifurcations of the fault. However, other faults were difficult to observe on the ground. Although we interpret traces to continue through this region they are not exposed because of heavy monsoon and glacial related erosion along the Dhaulagiri Front, a low slip magnitude making identification difficult, or older activations. The system is treated as primarily a single trace from Dogari Valley southward but further field mapping in the region northeast of the main observed trace is necessary to establish the presence of secondary features.

Atop the ridge where the main trace is visible above tree line are three subparallel valleys draining north to south with sharp ridges between them (Figure 15). They are

Figure 15. Satellite imagery of the Dogari Oblique Segment. Fault trace in red with normal and dextral kinematics. Offset ridges (A-C) between north to south glacially carved valleys. Normal slip on the fault trace has developed in the two western valleys to create Pond 1 and Pond 2. Note: Extrapolated ridge segments for slip estimation, straight sides of ponds against scarp face, and secondary ridges on protruding wings. The eastern valley does not exhibit the standing water as seen in the other two valleys, nor is its eastern ridge offset. Inset of dextral shoulders (Figure 18) is boxed in white.

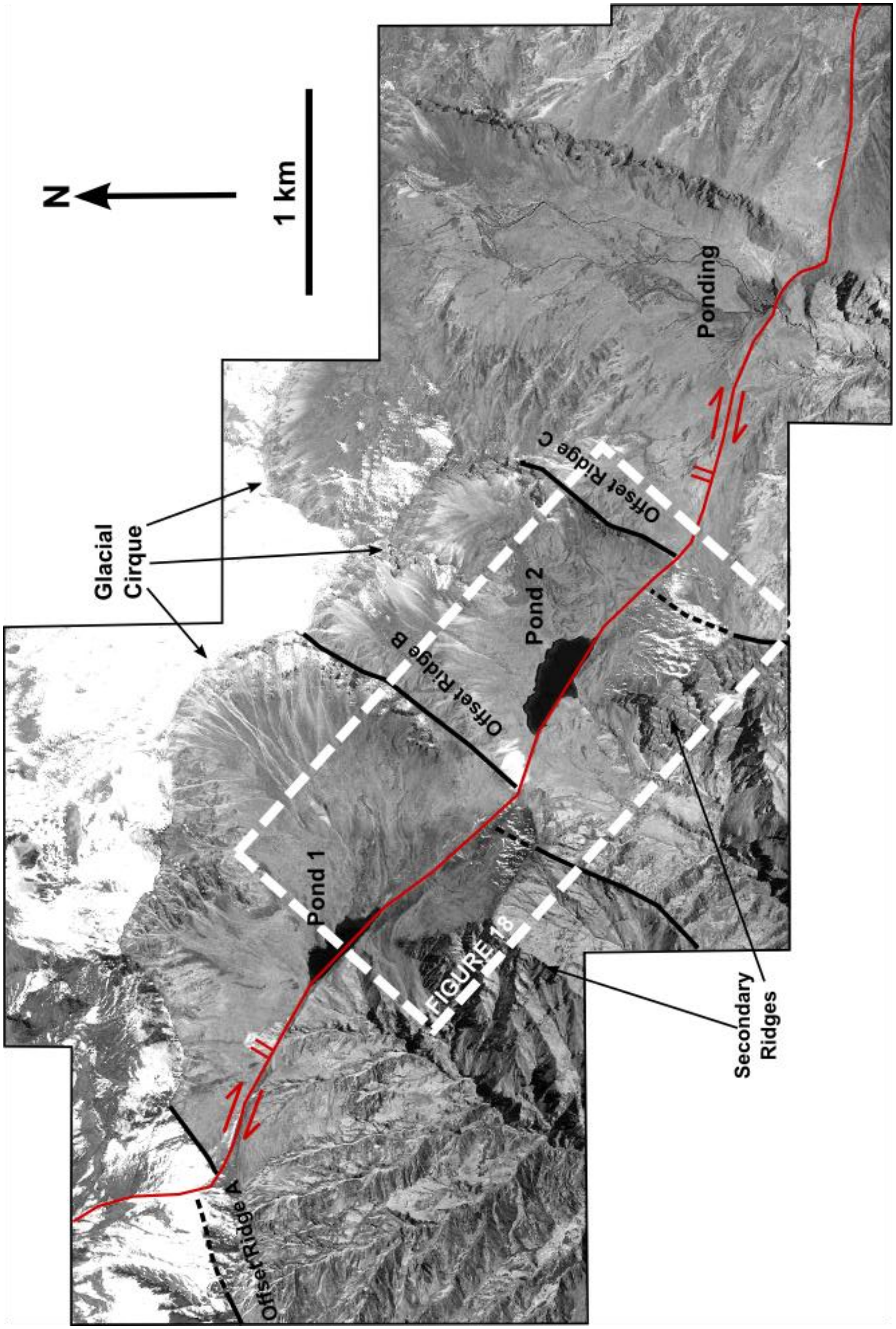
N
1 km
Glacial Cirque
Ponding
Offset Ridge C
Pond 2
Offset Ridge B
Pond 1
FIGURE 18
Secondary Ridges
Offset Ridge A

interpreted to be glacially derived due to the presence of extensive basal scoured lineations observed through grassy plain, poorly sorted angular boulders with glacial scouring on individual surfaces, distinct moraine deposits along the length of the valleys, and the glacial cirques at the apex of each of the valleys. Periglacial loess deposits blanket these valleys growing fine grasses intermingled with the rock debris.

These three valleys are crosscut by the fault, generating a number of Quaternary geomorphic features (Figure 15). The most striking features are two ponds, Pond 1 in the west is 380 meters at its widest and Pond 2 in the east is 420 meters. These ponds have developed along the scarp face due to dammed drainages. These ponds are ~5-10 m deep. The third valley has no standing water due to a developed drainage outlet through the raised scarp.

The primary fresh scarp obliquely cuts across LHC foliation at ~20˚ (Figure 16). The primary scarp dips ~50˚-60˚ to the NE, steeper than the foliation, with grasses growing on the surface and small debris exposures.

The scarp crest, throughout the area, is sharp with little to no erosion, even in the base of the glacial valley. Secondary scarp faces can be seen only on the high edges of the valley with changes in grass growth, boulder deposits, and crest erosion. They also exhibit a difference in strike from foliation but have a lower dip. Tertiary scarp faces, of similar strike but steeper dip, are possibly present, but difficult to map due to heavy erosion and debris coverage (Figure 16).

Figure 16. Field photo of Pond 1 in the Dogari region. Fault trace in red against interpreted scarp surfaces. 1-Primary scarp, 2-secondary scarp, 3-tertiary scarp, FOL-foliation layers with 20˚-25˚ difference in strike from foliation. Glaciation would have travelled from left to right. Note: sharp scarp crest and differential height of scarp, higher on the margins of the valley, lower in the middle.

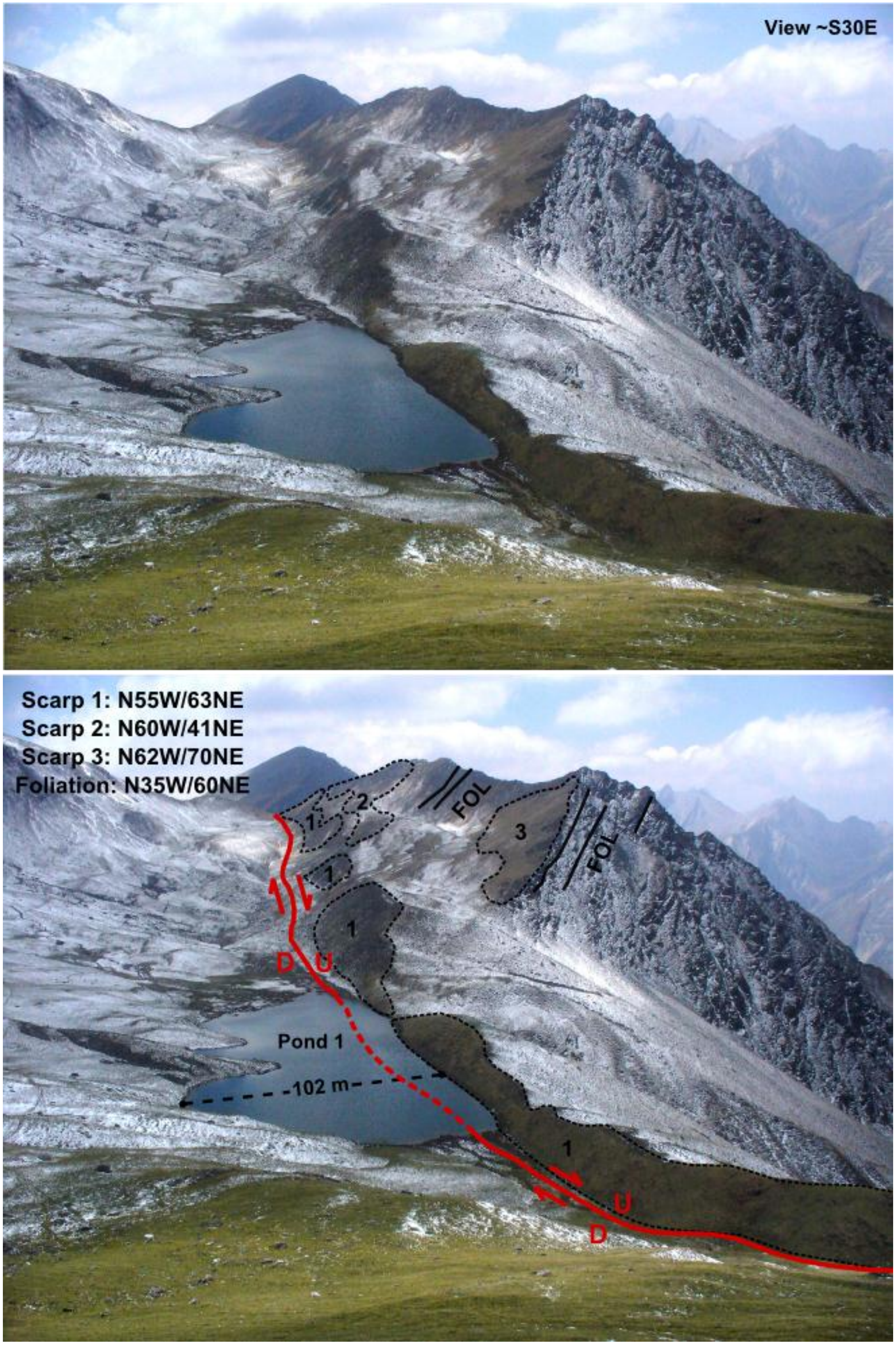
View ~S30E
Scarp 1: N55W/63NE
Scarp 2: N60W/41NE
Scarp 3: N62W/70NE
Foliation: N35W/60NE
FOL
FOL
1
2
3
D
U
Pond 1
102 m
U
D

Surfaces separated by the fault trace were correlated on the basis of debris type and offset scouring marks within the valley base. The height of the primary scarp is 31 m at the valley edges and 6 m adjacent to the ponds.

A high water mark is observed 1.5 m above the surface of the eastern pond during field work in early June (Figure 17). No grasses grow below this high water line though several loess deposits exist on the now exposed banks. No growth on this highly fertile loess, while it is carpeted by fine grass everywhere else, suggests that this high water mark is attained at regular intervals due to insufficient drainage. Sustained ponding due to poor drainage incision is corroborated by large quantities of green algae growing in both lakes, suggesting that these ponds do not dry often or have never dried completely. This implies that stream incision through the scarp is still developing, not allowing for complete drainage. Sustained ponding, low incision in an area hit regularly by the monsoon, sharp scarp crests, and fault-controlled primary scarp faces all point to Quaternary activity along this fault segment.

Dextral separation of the primary ridges bounding the glacial valleys is observed in satellite imagery (Figure 15). Correlation of the ridges shows a dextral offsets (Ridge A-C respectively) at 152 m, 180 m, and 163 m. These values are obtained by extrapolation of straight ridge lines to the interpreted fault trace. In this extrapolation we disregard the possibility of previous bends in the ridge lines. By again utilizing the minimum and maximum of the averaged values we provide an average dextral offset of 165 ± 15 meters in the Dogari region.

Figure 17. Field photo along the shore of Pond 2. High water mark of pond is noted in white. Shore is made up of gravely deposit and periglacial loess with no growth. Scarp 1 (30 m in height) and 3 are visible in the background though no scarp 2 is observed on the Pond 2 valley.


View ~S35E

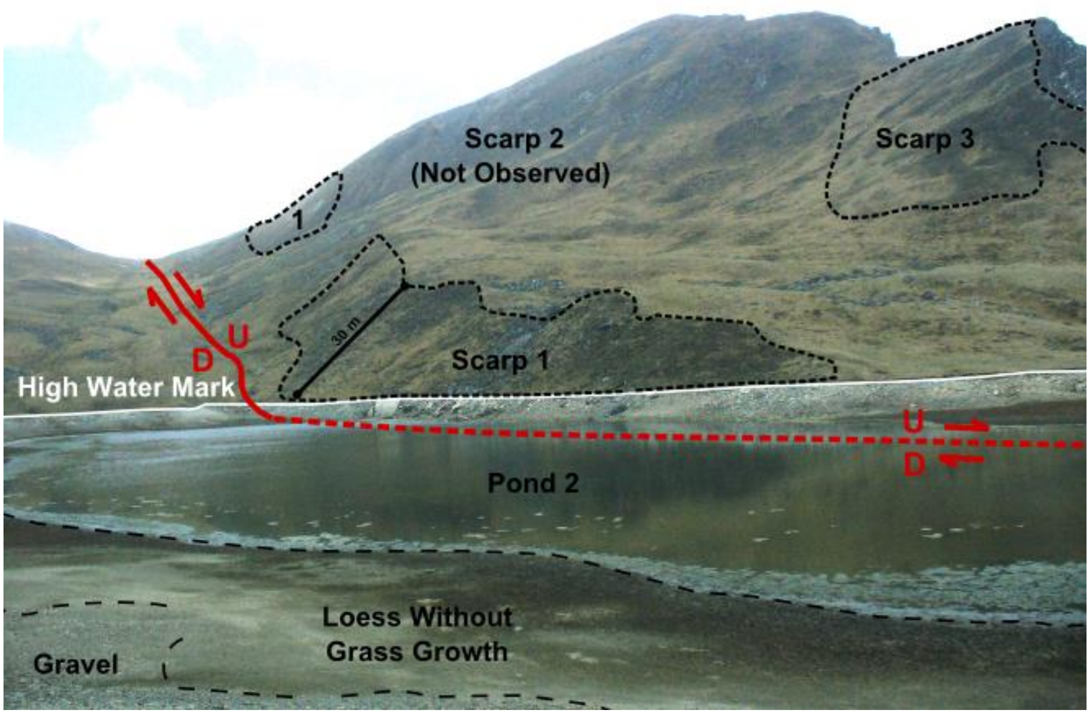
Scarp 2
(Not Observed)
1
Scarp 3
30 m
U
D
Scarp 1
High Water Mark
U
D
Pond 2
Loess Without
Grass Growth
Gravel

With this dextral value in mind it is possible to make other, though less conservative, correlations.

In the footwall between the two ponding valleys a secondary ridge is present and strikes subparallel to those used for the primary correlation above. This ridge sits atop a shoulder of rock which protrudes into the glacial valley (Figure 15). A similar shoulder of protruding rock is present on the eastern ridge as well, though the secondary ridge here is less distinct.

If these shoulders are a result of dextral motion, as is suggested by the secondary ridges, we can reconstruct these ridge lines to obtain offsets of ~464 m and ~414 m respectively. This would be a maximum measureable dextral offset of 439 ± 25 meters (Figure 18). The dip-slip distance between these hanging wall and footwall ridge features is less than 100 m and can be attributed to apparent slip of the protrusion of the valley sides, as well as erosion. This suggests Dogari to be a primarily strike-slip system with the exception of the primary scarp visible in the valley base.

The range of strike-slip offsets observed in the Dogari region can be attributed to a number of different processes. The most likely is that fault motion initiated prior to glaciation. The shoulders show glacial rounding on the leading edges suggesting dextral movement while a glacier was present. However, moraines draping both wings appear to be normally offset by the primary scarp with little to no significant dextral component to the separation (Figure 18).

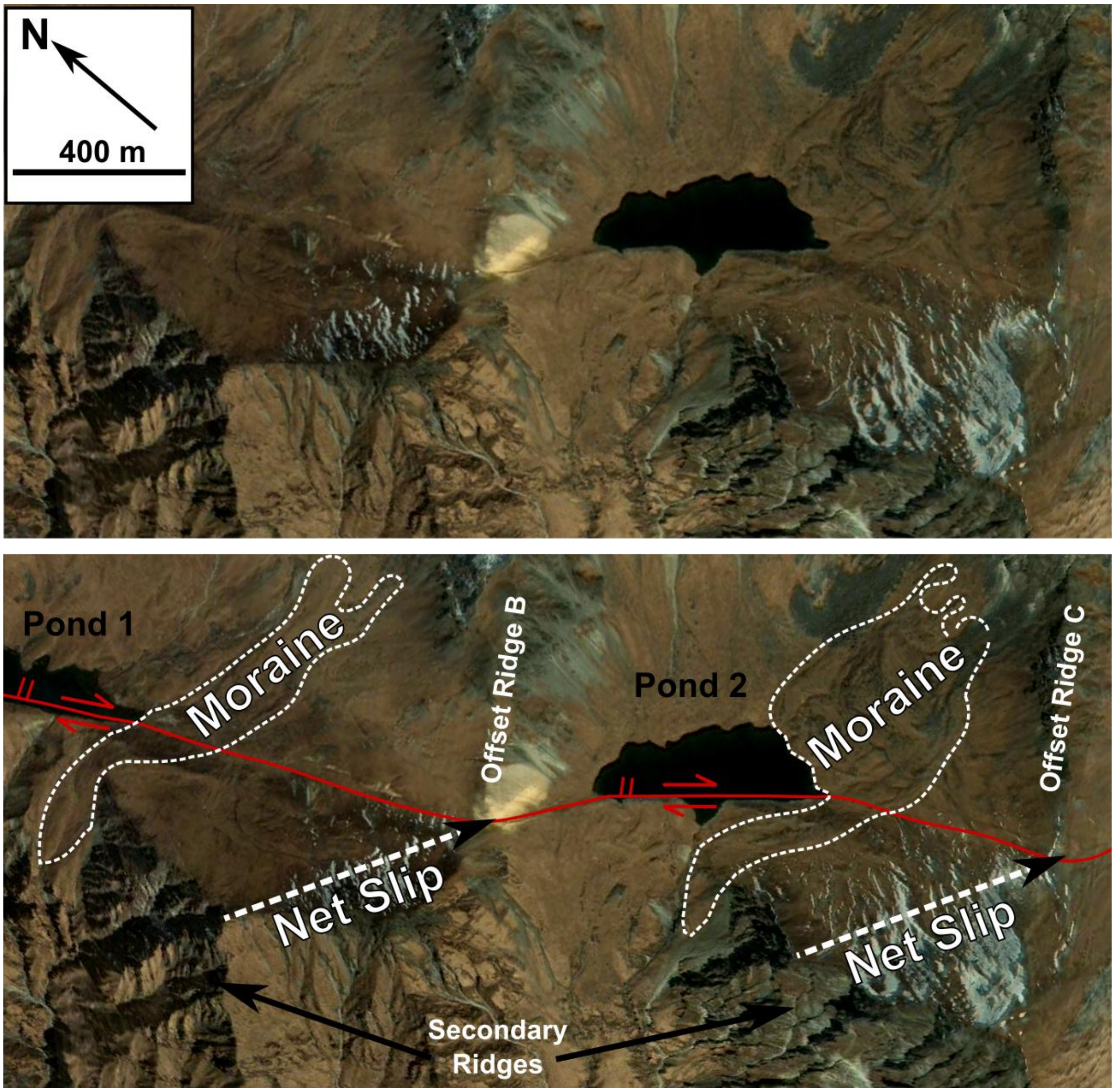

Figure 18. Satellite imagery of dextral shoulders protruding into the valleys associated with Pond 1 and 2. Offset of ridges B and C can be interpreted differently by using the secondary ridges for correlation. Moraine deposits drape both dextral wings.

Normal slip prior to or during glaciation would effectively erase scarp evidence in the valleys. The presence of the relatively uneroded 6 m primary scarp in the base of the glacial valley suggests motion since glaciation was last active (Figure 16). Six m of dip slip activity post glaciation is corroborated by the normally separated glacial moraine deposits next to Pond 1, Pond 2, and in the eastern valley (Figure 18). This attests to recent normal offset in this region since the last glacial maximum at 18 ka (Khule et al., 2005) but potentially much younger.

The trace continues N50W across Kape Valley to the ridge west of Dhaula Valley. The scarps mapped in Kape Valley are the northern most extent of the previously recognized Dhaulagiri Southwest Fault (Nakata 1989, 1990). The Dogari Oblique trace is interpreted to link directly to the DSWF which continues southeast with unverified kinematics. The village of Gurjagoan was the south and eastern most extent of the fault trace mapped in the field for this study.

The Dhaulagiri Transtensional Zone

In summary, the DTZ is an active fault system striking ~N50W across the Dhaulagiri Himalaya linking the Tibrikot Fault to the Dhaulagiri Southwest Fault. Dextral motion is transferred southward from the subvertical Tibrikot fault across a distributed N-S oriented, E-dipping extensional step over zone to an ~N50W striking, NE-dipping oblique fault (Figure 2 and 19). The DTZ exhibits a diffuse accommodation zone with decreasing dextral slip and increasing normal slip from NW to SE. Quaternary activity is interpreted via the faults crosscutting relationships with Quaternary features throughout its 80 km extent.

DISCUSSIONS

DLP0 GPS Arc-parallel Vector Decompositions

GPS data from station DLP0, 2 km south of Tibrikot and 11 km northwest of Gumbagoan, yields a Himalaya arc-parallel (N57W) velocity of 5.71 ± 2.25 mm yr^{-1} as presented in Styron et al. (2011). This study found the geodetic motion to be subparallel to the previously mentioned Tibrikot Fault. The Tibrikot Fault was thus interpreted to primarily accommodate arc-parallel motion via dextral slip on a subvertical surface as is suggested of the arc-parallel system as a whole, from the Karakoram Fault southward. The Gumbagoan Extensional Step-over links to Tibrikot and in-turn also accommodates arc-parallel motion. The orientation of the Gumbagoan system, N10-20E, in relation to the geodetic station at Tibrikot, geometrically suggests three times more dip-slip movement than dextral motion for this fault segment (Figure 19). This supports the observations and interpretation of a normal fault system with little dextral slip observed on visible traces acting as an extensional step-over in a larger regional strike-slip fault system.

Due to linkage between the Jangla Oblique Segment to the Gumbagoan Extensional Step-over it is possible to do a vector decomposition of the GPS data from DLP0.

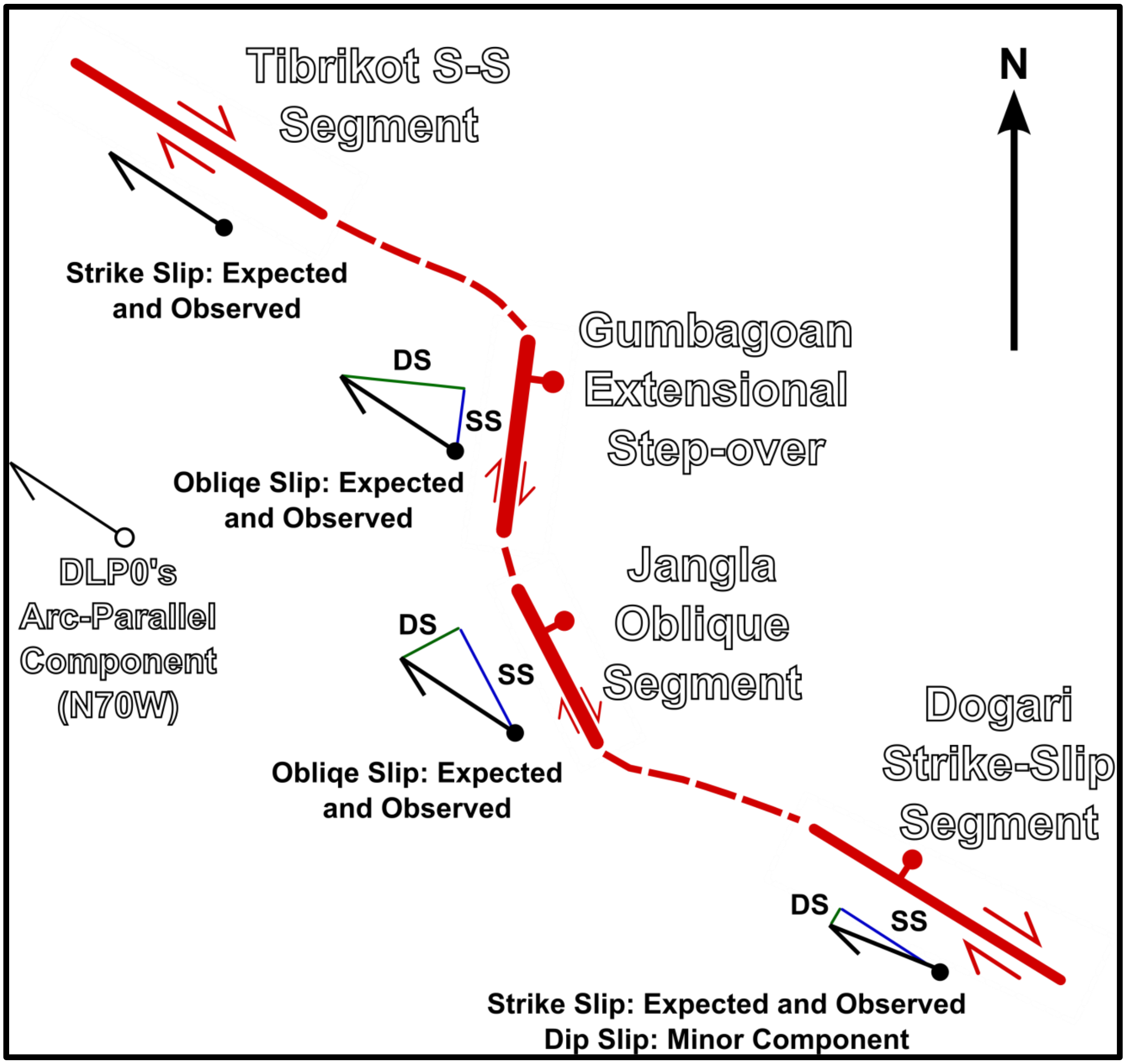

Figure 19. Regional satellite imagery of the DTZ with the four neotectonic segments simplified geometry. Geodetic station DLP0 (Styron et al., 2011) resides near the villages of Tibrikot and Juphal. Decompositions of this vector have been shown for all four locations. Note: pure dextral slip is predicted at the Dogari Segment; however, a decrease in dextral slip is seen as well as a prominent normal slip motion.

Here (striking N20W), dextral strike-slip motion and dip slip motion are approximately one-to-one with dextral motion being slightly more dominant. The observed dip-slip magnitude is ambiguous in the Jangla region as previously stated, but the resumption of significant dextral motion is indicated by our field measurements.

The Dogari Oblique Segment has a fault orientation subparallel to Tibrikot. Dextral motion is expected on a fault oriented similar to Tibrikot, but the magnitude of dextral slip observed at Dogari is less. The presence of a recent dip-slip scarp is not observed at Tibrikot as is seen at Dogari. This suggests that the majority of motion in Dogari can be attributed to the DLP0 arc-parallel vector, but that a slight arc-normal component is also present in this region.

The change from little to no dip slip and 649 ± 219 m dextral slip at the Tibrikot Fault to 165-450 m dextral slip and minor dip slip at Dogari is predicted by perfect transfer of arc-parallel motion with the slight inclusion of arc-normal kinematics in the southwest. The difference in kinematics and magnitude of slip across the DTZ indicates a decrease in arc-parallel motion from west to east across the fault. An increase in dip slip activity is observed which may correlate to an increase in arc-normal strain near the southern extent of the DTZ.

Structural Linkages

The previously mentioned system of structures linking the Karakoram Fault Zone to the Tibrikot Fault shows a decrease in arc-parallel slip from northwest to southeast. As stated above the DTZ continues this trend as it transfers slip further southeast to the Central Himalaya.

The DTZ is interpreted to link with the Dhaulagiri Southwest Fault (Nakata 1989, 1990). The DSWF likely accommodates oblique slip similar to that seen in the Dogari Segment and subsequently transfers this movement into the region south of Thakkhola Graben which is characterized by arc-normal strain (Hurtado et al., 2001; Wobus et al., 2003, 2005; Hodges et al., 2004; McDermott et al., 2009).

Similarities and linkages between the Dhaulagiri Himalaya and Central Himalaya have been established in previous studies. The westernmost structure previously assessed in the Thakkhola region is the Larjung Detachment (McDermott et al., 2009) which is interpreted to accommodate some amount of dextral slip and lies structurally ~2 km above the STDS. Hurtado et al. (2001) interpreted a link between the active Dhumpu Detachment and the DSWF at its eastern end. If the DTZ links with the DSWF at its western end this would effectively tie the DTZ, and the chain of arc-parallel structures, with a modern STDS activation.

These geometrically and kinematically similar faults sit at a similar structural level, suggesting a 350 km long right slip system linking the Karakoram Fault Zone to the Central Himalaya.

Western Nepal Kinematic Transition

Based on the structural linkages interpreted in this study and others, the Dhaulagiri Transtensional Zone can be considered as a transitional system linking arc-parallel strain in northwest Nepal and the arc-parallel and arc-normal strain in the Central Himalaya.

The DTZ is indicative of the most recent deformation processes in the western Nepal High Himalaya. Likely postdating all active structures in the region, the DTZ is a factor in understanding orogenic behavior in the High Himalaya of Nepal at a local and regional scale.

Development of this modern system speaks to the active and significant nature of the differing structures bounding it to the east and west. Primary accommodation of dextral motion, as well as the minor presence of dip-slip activity, implies arc-parallel stresses are acting on the system as a majority with some component of arc-normal stress being worked in either synkinematically or cyclically at this stage in the growth of the Himalaya Orogen.

Strain Partitioning in Convergent Orogens

While the DTZ likely acts as a transition between differing kinematics to the west and east, the regional right-slip system, from the Karakoram Fault Zone to the DSWF, lies between active N-S compression along the MFT/MBT and E-W extension of Tibet. Thus this regional system acts as a margin between these two developmental processes of orogenic growth, acting as a buffer between both styles of deformation along a regionally extensive zone of oblique faulting.

This partitioning of deformation is observed at obliquely convergent margins, both continental and oceanic.

Global corollaries exhibit similar faulting morphology to the Himalaya's strike-slip faults. A developing example, the Zagros Mountains transfers dextral slip from the northwestern Main Recent Fault to the more modernly initiated Kazerun Fault which links to the Mountain Flexural Front, similar to the MBT of the Himalaya (Authemayou et al., 2006; Hessami et al., 2007). This suggests the Karakoram Fault Zone links to the Himalaya's thrust front via the arc-parallel system.

Conversely, a more mature system, the Longitudinal Valley Fault of Taiwan is suggested to accommodate all strain generated by oblique convergence between the Philippines Sea Plate and Eurasia. This sub-discrete sinistral structure acts seemingly independent of the rest of the convergent margin in Taiwan (Lee et al., 1998; Beih et al., 1990; Yu and Kuo, 2001; Shyu et al., 2006; Shyu et al., 2008).

With this in mind, the right-slip system as a whole could be a short lived distributed fault zone which will eventually evolve into some through going discrete system cutting across Western Nepal and the Dhaulagiri Himalaya. It could directly link arc-parallel strain with arc-normal strain. However, the through-going structure could continue toward the MFT/MBT, thus generating a distinct fore-arc sliver (e.g. Beck, 1983, 1986, 1991; Jarrad, 1986; Kimura, 1986; Apel et al., 1998; Chemenda et al., 2000; Upton et al., 2003; McClay et al., 2004; Haq and Davis, 2010). Fore-arc slivers separate from the arc along vertical strike-slip faults at convergent margins. This sliver separation allows for the accommodation of oblique motion of convergence with minimal friction while detachment and thrust horizons, higher in surface area and prevalent in the Himalaya, move in a purely dip slip fashion (Michael, 1990).

CONCLUSIONS

The primary results of this study are:

1. Two strike-slip segments are linked by an extensional step over in the high Dhaulagiri Himalaya, termed the DTZ.
2. Fault scarp morphology, geomorphology, and Quaternary offsets suggest the fault is younger than the last glacial maximum.
3. A decrease in dextral slip and an increase in normal slip is observed from NW to SE across the fault's extent.
4. This recent fault system can be correlated with strike-slip structures in SW Nepal to the central Himalaya; thus, suggesting a regionally extensive right-slip system.
5. We speculate that this system, as a whole, acts as a buffer zone between N-S strain in the Himalayan front and E-W extension within the Tibetan Plateau.
6. This suggests the presence of an "isolated" structural block (forearc sliver) within the Nepal Himalaya.

REFERENCES CITED

Apel, E.V., Burgmann, R., and Banerjee, P., 2008, Indian Plate motion, deformation, and plate boundary interactions: Eos (Transactions, American Geophysical Union), Fall Meeting 2008, abs. G34A-01.

Armijo, R., Tapponnier, P., Mercier, J., and Tong-Lin, H., 1986, Quaternary extension in southern Tibet: Field observations and tectonic implications: Journal of Geophysical Research, v. 91, p. 13,803–13,872, doi: 10.1029/JB091iB14p13803.

Armijo, R., Tapponnier, P., and Tonglin, H., 1989, Late Cenozoic right-lateral strike-slip faulting in southern Tibet: Journal of Geophysical Research, v. 94, p. 2787-2838.

Authemayou, C., Chardon, D., Bellier, O., Malekzadeh, Z., Shabanian, E., and Abbassi, M.R., 2006, Late Cenozoic partitioning of oblique plate convergence in the Zagros fold-and-thrust belt (Iran): Tectonics, v. 25, doi: 10.1029/2005TC001860.

Avouac, J.P., Dobremez, J.F., and Bourjot, L., 1996, Palaeoclimatic interpretation of a topographic profile across middle Holocene regressive shorelines of Longmu Co (Western Tibet): Palaeogeography, Palaeoclimatology, Palaeoecology, v. 120, p. 93–104.

Barrier, E., Huchon, P., and Aurelio, M., 1991, Philippine Fault: A key for Philippine kinematics: Geology, v. 19, p. 32-35.

Beck, M.E., 1983, On the mechanism of tectonic transport in zones of oblique subduction: Tectonophysics, v. 93, p. 1-11.

Beck, M.E., 1986, Model for late Mesozoic-early Tertiary tectonics of coastal California and Western Mexico and speculations on the origin of the San Andreas Fault: Tectonics, v. 5, p. 49-64.

Beck, M.E., 1991, Coastwise transport reconsidered: Lateral displacements in the oblique subduction zones, and tectonics consequences: Physical Earth and Planetary Interiors, v. 68, p. 1-8.

Beih, Y.S., Jackson, D.D., Guey-Kuen, Y., and Chi-Ching, L., 1990, Dislocation model for crustal deformation in the Longitudinal Valley area, Eastern Taiwan: Tectonophysics, v. 183, p. 97-109.

Braun, J., and Beaumont, C., 1995, Three-dimensional numerical experiments of strain partitioning at oblique plate boundaries: Implications for contrasting tectonic styles in the Southern Coast Ranges, California, and Central South Island, New Zealand: Journal of Geophysical Research, v. 100, p. 18,059-18,074.

Brown, R.L., and Nazarchuk, J.H., 1993, Annapurna detachment fault in the Greater Himalaya of central Nepal: The Journal of the Geological Society, London, Special Publications, v. 74, p. 461-473.

Burg, J.P., Brunel, M., Gapais, D., Chen, G.M., and Liu, G.H., 1984, Deformation of the crystalline Main Central Sheet in southern Tibet (China): Journal of Structural Geology, v. 6, p. 535-542.

Carosi, R., Montomoli, C. and Visonà, D., 2007, A structural transect in the Lower Dolpo: Insights on the tectonic evolution of Western Nepal: Journal of Asian Earth Sciences, v. 29, p. 407–423.

Chemenda, A., Lallemand, S., and Bokun, A., 2000, Strain partitioning and interpolate friction in oblique subduction zones: Constraints provided by experimental modeling: Journal of Geophysical Research, v. 105, p. 5567-5581.

Chen, Q., Freymueller, J.T., Yang, Z., Xu, C., Jiang, W., Wang, Q., and Liu, J., 2004, Spatially variable extension in southern Tibet based on GPS measurements: Journal of Geophysical Research, v. 109, doi:10.1029/2002JB002350.

Cogan, M.J., Nelson, K.D., Kidd, W.S.F., Wu, C., and Project, I.T., 1998, Shallow structure of the Yadong- Gulu rift, southern Tibet, from refraction analysis of Project INDEPTH common midpoint data: Tectonics, v. 17, p. 46–61, doi: 10.1029/97TC03025.

Colchen, M., 1980, Evolution paléogéographique et structural du fossé de la Thakkhola-Mustang (Himalaya du Népal): Implications sur l'histoire récente de la chaîne himalayenne: Paris, Comptes Rendus des Académie des Sciences, v. 290, p. 311–314.

Colchen, M., Le Fort, P., and Pêcher, A., 1986, Annapurna–Manaslu–Ganesh Himal: Paris, Centre National de la Recherche Scientifique, 136 p. Scale 1:200,000.

Coleman, M.E., 1996, Orogen-parallel and orogen-perpendicular extension in the central Nepalese Himalayas: Geological Society of America Bulletin, v. 108, p. 1594–1607.

Dewane, T., Stockli, D., Hager, C., Taylor, M., Ding, L., Lee, J., and Wallis, S., 2006, Timing of Cenozoic E-W extension in the Tangra Yum Co-Kung Co Rift, southcentral Tibet: Eos (Transactions, American Geophysical Union), v. 87, no. 52, fall meeting supplement, abs. T34C–04.

Dunlap, W.J., Weinberg, R.F., and Searle, M.P., 1998, Karakoram fault zone rocks cool in two phases: Journal of the Geological Society, London, v. 155, p. 903-912.

Ekström. G., and Engdahl, P., 1989, Seismic strain rates in regions of distributed continental deformation: Journal of Geophysical Research, v. 94, p. 10,231-10,257.

Glodny, J., Lohrmann, J,. Echtler, H., Gräfe, K., Seifert, W., Collao, S., and Figueroa, O., 2005, Internal dynamics of the paleoaccretionary wedge: Insights from combine isotope tectonochronology and sandbox modeling of the South-Central Chilean fore-arc: Earth and Planetary Science Letters, v. 231, p. 23-29.

Godin, L., 2003, Structural evolution of the Tethyan sedimentary sequence in the Annapurna area, central Nepal Himalaya; Journal of Asian Earth Sciences, v. 22, p. 307-+.

Godin, L., Brown, R.L., Hanmer, S., and Parrish, R., 1999, Back folds in the core of the Himalayan orogen: An alternative interpretation: Geology, v. 27, p. 151-154.

Griffiths, P.S., 1980, Box fault systems and ramps: a typical association of structures from the eastern shoulder of the Kenya Rift: Geological Magazine, v. 117, p. 579-586.

Hager, C., Stockli, D., Dewane, T., Ding, L., Taylor, M., and Lee, J., 2006, Episodic Mio-Pliocene rifting in southcentral Tibet. Thermochronometric constraints from the Xainza rift: Eos (Transactions, American Geophysical Union), v. 87, no. 52, fall meeting supplement, abs. T34C–02.

Haq, S.S., and Davis, D.M, 2010, Mechanics of fore-arc slivers: Insight from simple analog models: Tectonics, v. 29, doi: 10.1029/2009TC002583.

Hessami, K., Koyi, H.A., and Talbot, C.J., 2007, The significance of strike-slip faulting in the basement of the Zagros fold and thrust belt: Journal of Petroleum Geology, v. 24, p. 5-28.

Hodges, K.V., Parrish, R., Housh, T., Lux, D., Burchfiel, B.C., Royden, L., and Chen, Z., 1992, Simultaneous Miocene extension and shortening in the Himalayan orogen: Science, v. 258, p. 1466–1470.

Hodges, K., Bowring, S., Davidek, K., Hawkins, D., and Krol, M., 1998, Evidence for rapid displacement on Himalayan normal faults and the importance of tectonic denudation in the evolution of mountain ranges: Geology, v. 26, p. 483–486.

Hodges, K.V., Wobus, C., Ruhl, K., Schildgen, T., and Whipple, K., 2004, Quaternary deformation, river steepening, and heavy precipitation at the front of the Higher Himalayan ranges: Earth and Planetary Science Letters, v. 220, p. 379-389.

Hubbard, M.S., 1989, Thermobarometric constraints on the thermal history of the Main Central Thrust Zone and Tibetan Slab, eastern Nepal Himalaya: Journal of Metamorphic Geology, v. 7, p. 19–30.

Hurtado, J.M., Hodges, K.V., and Whipple, K.X., 2001, Neotectonics of the Thakkhola graben and implications for recent activity on the South Tibetan fault system in the central Nepal Himalaya: Geological Society of America Bulletin, v. 113, p. 222-240.

Jackson, J., and Molnar, P., 1991, Active faulting and block rotations in the Western Traverse Ranges, California: Journal of Geophysical Research, v. 96, p. 22,073-22,087.

Jarrad, R.D., 1986, Relations among subduction parameters: Reviews of Geophysics, v. 24, p. 217-284.

Jones, C.H., and Wesnousky, S.G., 1992, Variations in strength and slip rate along the San Andreas Fault System: Science, v. 256, p. 83-86.

Kapp, P., DeCelles, P.G., Gehrels, G.E., Heizler, M., and Ding, L., 2007, Geological records of the Lhasa-Qiangtang and Indo-Asian collisions in the Nima area of central Tibet: GSA Bulletin, v. 119, p. 917-933.

Kimura, G., 1986, Oblique subduction and collision: Fore-arc tectonics of the Kuril Arc: Geology, v. 14, p. 404-407.

Khule, M., 2005, Glacial geomorphology and ice in Tibet and the surrounding mountains: The Island Arc, v. 14, 346-367.

Lacassin, R., Valli, F., Arnaud, N., Leloup, P.H., Paquette, J.L., Li, H., Tapponnier, P., Chevalier, M.-L., Guillot, S., Maheo, G., and Xu, Z., 2004, Large-scale geometery and offset of the Karakoram fault, Tibet: Earth and Planetary Science Letters, v. 219, p. 255-269.

Larson, K., Burgmann, R., Bilham, R., and Freymueller, J.T., 1999, Kinematics of the India-Eurasia Collision Zone from GPS measurements: Journal of Geophysical Research.

Lavé and Avouac, 2000 Lavé, J., and Avouac, J.P., 2000, Active folding of fluvial terraces across the Siwaliks Hills, Himalayas of central Nepal: Journal of Geophysical Research, v. 105, no. B3, p. 5735–5770, doi: 10.1029/1999JB900292.

Lee, J., Angelier, J., Chu, H., Yu, S., and Hu, J., 1998, Plate-boundary strain partitioning along the sinistral collision suture of the Philippine and Eurasian plates: Analysis of geodetic data and geological observation in southeastern Taiwan: Tectonics, v. 17, p. 859-871.

Lee, J., Hager, C., Wallis, S.R., Stockli, D.F., Whitehouse, M.J., Aoya, M., and Wang, Y., 2011, Middle to late Miocene extremely rapid exhumation and thermal reequilibriation in the Kung Co rift, southern Tibet: Tectonics, doi: 10.1029/2010TC002745, (in press).

Le Fort, P., 1975, Himalayas: The collided range. Present knowledge of the continental arc: American Journal of Science, v. 275, p. 1–44.

Mahéo, G., Leloup, P.H., Valli, F., Lacassin, R., Arnaud, N., Paquette, J.L., Fernandez, A., Haibing, L., Farley, K.A., and Tapponnier, P., 2007, Post 4 Ma initiation of normal faulting in southern Tibet. Constraints from the Kung Co half graben: Earth and Planetary Science Letters, v. 256, p. 233–243, doi: 10.1016/ j.epsl.2007.01.029.

Malik, N.J., and Nakata, T., 2003, Active faults and related Late Quaternary deformation along the Northwest Himalaya Frontal Zone, India: Annals of Geophysics, v. 46, p. 917-936.

McCaffrey, R., 1991, Slip vectors and stretching of the Sumatran Fore Arc: Geology, v. 19, p. 881-884.

McCaffrey, R., 2009, The tectonic framework of the Sumatran subduction zone: Annual Review of Earth and Planetary Sciences, v. 37, p. 345-366.

McCaffrey, R., and Nábelek, J., 1998, Role of oblique convergence in the active deformation of the Himalayas and southern Tibet plateau: Geology, v. 26, p. 691-694.

McClay, K.R., Whitehouse, P.S., Dooley, T., and Richards, A., 2004, 3D evolution of fold and thrust belts formed by oblique convergence: Marine Petroleum Geology, v. 21, p. 857-877.

McDermott, J., Hodges, K., and van Soest, M., 2009, Polyphase (Miocene-Pleistocene?) slip on the South Tibetan Fault system in the Dhaulagiri Himalaya: *in* Proceedings, EOS Transactions San Francisco, v. 90, AGU.

Meigs, A.J., Burbank, D.W., and Beck, R.A., 2005, Middle-late Miocene (>10 Ma) formation of the Main Boundary thrust in the western Himalaya: Geology, v. 23, p. 423-426.

Melnick, D., Bookhagen, B., Strecker, M.R., and Echtler, H.R., 2009, Segmentation of the megathrust rupture zones from fore-arc deformation patterns over hundreds of millions of years, Arauco peninsula, Chile: Journal of Geophysical Research, v.114, dio: 10.1029/2008JB005788.

Michael, A.J., 1990, Energy constraints on kinematic models of oblique faulting: Loma-Prieta versus Parkfield-Coalinga: Geophysical Research Letters, v. 17, p. 1453-1456.

Molnar, P., 1992, Mountain building - crust in mantle overdrive: Nature, v. 358, p. 105-106.

Moreno, M., Klotz, J., Melnick, D., Echtler, H.P., and Bataille, K., 2008, Contemporary forearc deformation in south-central Chile from GPS observations (36-39˚S): 7th International Symposium on Andean Geodynamics, Nice, France, Extended Abstracts, p. 348-350.

Mount, V.S., and Suppe, J., 1987, State of stress near the San Andreas Fault: Implications for wrenching tectonics: Geology, v. 15, p. 1143-1146.

Murphy, M.A., Yin, A., Kapp, P., Harrison, T.M., Lin, D., and Guo, J.H., 2000, Southward propagation of the Karakoram fault system, southwest Tibet: Timing and magnitude of slip: Geology, v. 28, p. 451-454.

Murphy, M.A., Yin, A., Kapp, P., Harrison, T.M., Manning, C.E., Ryerson, F.J., Lin, D., and Jinghui, G., 2002, Structural evolution of the Gurla Mandhata detachment system, southwest Tibet: Implications for the eastward extent of the Karakoram fault system: Geological Society of America Bulletin, v. 114, p. 428-447.

Murphy, M.A., Sanchez, V., and Taylor, M.H., 2010, Syncollisional extension along the India-Asia suture zone, south-central Tibet: Implications for crustal deformation of Tibet: Earth and Planetary Science Letters, v. 290, p. 233–243, doi: 10.1016/j.epsl.2009.11.046.

Murphy, M.A., and Burgess, W.P., 2006, Geometry, kinematics, and landscape characteristics of an active transtension zone, Karakoram fault system, Southwest Tibet: Journal of Structural Geology, v. 28, p. 268-283.

Murphy, M.A., and Copeland, P., 2005, Transtensional deformation in the central Himalaya and its role in accommodating growth of the Himalaya orogen: Tectonics, v. 24, TC4012, doi: 10.1029/2004TC001659.

Nakata, T., 1975, On Quaternary tectonics around the Himalayas: Scientific Reports Tohoku University, v. 22, p. 111-118.

Nakata, T., 1989, Active faults of the Himalaya and India and Nepal: Geological Society of America Special Publications, v. 232, p. 243-264.

Nakata, T., Otsuki, K., and Khan, S.H., 1990, Active Faults, Stress-Field, and Plate Motion Along the Indo-Eurasian Plate Boundary: Tectonophysics, v. 181, p. 83-95

Phillips, R.J., Parrish, R.R., and Searle, M.P., 2004, Age constraints on ductile deformation and long-term slip rates along the Karakoram fault zone, Ladakh: Earth and Planetary Science Letters, v. 226, p. 305-319.

Rastchbacher, L., Frisch, W., and Liu, G., 1994, Distributed deformation in southern and western Tibet during and after the India-Asia collision: Journal of Geophysical Research, v. 99, p. 19917-19945.

Sanchez, V. 2011, Structural evolution of the Lopukangri rift, south-central Tibet: implications for intercontinental deformation, timing of extension of the Tibetan Plateau, and evolution of the Himalaya orogen and India-Asia suture zone. PhD thesis, University of Houston, Houston, Texas, 246 p.

Searle, M.P., Yeh, M.W., Lin, T.H., and Chung, S.L., 2010, Structural constraints on the timing of left-lateral shear along the Red River shear zone in the Ailao Shan and Diancang Shan Ranges, Yunnan, SW China: Geosphere, v. 6, p. 316-338.

Schelling, D., 1992, The tectonostratigraphy and structure of the eastern Nepal Himalaya: Tectonics, v. 11, p. 925-943.

Searle, M.P., 1996, Geological evidence against large-scale pre Holocene offsets along the Karakoram Fault: Implications for the limited extrusion of the Tibetan Plateau, Tectonics, v. 15, p. 171-186.

Searle, M.P., Weinberg, R.F., and Dunlap, W.J., 1998, Transpressional tectonics along the Karakoram fault zone, northern Ladakh: Constraints on Tibetan extrusion, *in* Holdsworth, R.E., et al., eds., Continental transpressional and transtensional tectonics. Geological Society of London Special Publication 135, p. 307– 326, doi: 10.1144/GSL.SP.1998.135.01.20.

Searle, M.P., Law, R.D., Godin, L., Larson, K.P., Streule, M.J., Cottle, J.M., and Jessum, M.J., 2008, Defining the Himalayan Main Central Thrust in Nepal: Journal of the Geological Society, v. 165, p. 523-534.

Seeber, L., and Pecher, A., 1998, Strain partitioning along the Himalayan arc and the Nanga Parbat antiform: Geology, v. 26, p. 791-794.

Shyu, J.B.H., Sieh, K., Avouac, J., Chen, W., and Chen, Y., 2006, Millennial slip rate of the Longitudinal Valley fault from river terraces: Implications for convergence across the active suture of eastern Taiwan: Journal Geophysical Research, v.111, doi: 10.1029/2005JB003971.

Shyu, J.B.H., Sieh, K., Chen, Y., Chuang, R.Y., Wang, Y., and Chung, L., 2008, Geomorphology of the southernmost Longitudinal Valley fault: Implications for evolution of the active suture of eastern Taiwan: Tectonics, v. 27, doi: 10.1029/2006TC002060.

Styron, R., and M. Taylor, M. Murphy**,** 2011, Oblique Convergence, Arc Parallel Extension, and Strike-Slip faulting in the High Himalaya, under review, Geosphere.

Tapponnier, P., and Molnar, P., 1979, Active faulting and Cenozoic tectonics of the Tien Shan, Mongolia, and Baykal regions: Journal of Geophysical Research, v. 84, 3425-3459, doi: 10.1029/JB084IB07P03425

Taylor, M., Yin, A., Ryerson, F., Kapp, P., and Ding, L., 2003, Conjugate strike-slip faults accommodate coeval north-south shortening and east-west extension along the Bangong-Nujiang suture zone in central Tibet: Tectonics, v. 22, 1044, doi: 10.1029/2002TC00136.

Taylor, M.H., and Peltzer, G., 2006, Current slip rates on conjugate strike-slip faults in central Tibet using synthetic aperture radar interferometry: Journal of Geophysical Research – Solid Earth, v. 111, no. B12.

Taylor, M., Kapp, P., Stockli, D., Murphy, M., Dewane, T., and Lin, D., 2007, Structural observations from the Tangra Yum Cu, Lunggar Shan, and Lopu-Kangri Rift Systems, Southern Tibet: American Geophysical Union, Fall Meeting, San Francisco, abs. T13H-05.

Taylor, M.H., Murphy, M.A., 2008, Active orogen parallel strike-slip faulting in the Lower Dolpa region, northwest Nepal: Implications for expansion of the Himalaya Arc: American Geophysical Union, Fall Meeting, San Francisco, abs. T41A-1949.

Taylor, M.H., and Yin, A., 2009, Active structures of the Himalayan-Tibetan orogen and their relationships to earthquake distribution, contemporary strain field, and Cenozoic volcanism: Geosphere, v. 5, p. 199-214.

Turner, H.L., LaFemina, P., Saballos, G., Mattioli, G.S., Jansma, E., and Dixon, T., 2007, Kinematics of the Nicaraguan forearc from GPS geodesy: Geophysical Research Letters, v. 34, doi:10.1029/2006GL027586.

Upton, P., Koons, P.O., and Eberhard-Phillips, D., 2003, Extensional and partitioning in an oblique subduction zone, New Zealand: Constraints from three-dimensional numerical modeling: Tectonics, v. 22, p. 1068.

Vannay, J.C., and Hodges, K., 1996, Tectonometamorphic evolution of the Himalayan metamorphic core between the Annapurna and Dhaulagiri, central Nepal: Journal of Metamorphic Geology, v.14, p.635-656.

Vernant, P., and Chéry, J., 2006, Mechanical modeling of oblique convergence in the Zagros, Iran: Geophysics Journal International, v. 165, p. 991-1002.

Walsh, J.J., and J. Watterson, 1991, Geometric and kinematic coherence and scale effects in normal fault systems, *in* A.M. Roberts, G. Yielding, and B. Freeman, eds., The geometry of normal faults: Geological Society of London, Special Publication, no. 56, p. 193-203.

Wobus, C.W., Hodges, K.V., and Whipple, K.X., 2003, Has focused denudation sustained active thrusting at the Himalayan topographic front?: Geology, v. 31, p. 861-864.

Wobus, C., Heimsath, A., Whipple, K., and Hodges, K., 2005, Active out-of-sequence thrust faulting in the central Nepalese Himalaya: Nature, v. 434, p. 1008-1011.

Yin, A., 2000, Mode of Cenozoic east-west extension in Tibet suggesting a common origin of rifts in Asia during the Indo-Asian collision: Journal of Geophysical Research, v. 105, no. B9, p. 21,745–21,759, doi: 10.1029/2000JB900168.

Yin, A., Harrison, T.M., Murphy, M.A., Grove, M., Nie, S., Ryerson, F.J., Wang, X.F., and Chen, Z.L., 1999, Tertiary deformation history of southeastern and southwestern Tibet during the Indo-Asian collision: GSA Bulletin, v. 111, no. 11, p. 1644-1664.

Yin, A., Kapp, P., Murphy, M., Manning, C.E., Harrison, T.M., Din, L., Xiguang, D., and Chunming, W., 1999, Significant late Neogene east-west extension in north Tibet: Geology, v. 27, p. 787–790, doi: 10.1130/ 0091-7613(1999)027<0787:SLNEWE>2.3.CO;2.

Yin, A., and Harrison, T.M., 2000, Geologic evolution of the Himalayan-Tibetan orogen: *Annual Review of Earth and Planetary Science*, v. 28, p. 211-280.

Yu, S., and Kuo, L., 2001, Present-day crustal motion along the Longitudinal Valley Fault, eastern Taiwan: Tectonophysics, v. 333, p. 199-217.

Zoback, M.D., et al., 1987, New evidence on the state of stress of the San Andreas Fault system: Science, v. 238, p. 1105-1111.